Journal of Medicinal Chemistry

pubs.acs.org/jmc

Article

Structure–Activity Relationship in the Leucettine Family of Kinase Inhibitors

Tania Tahtouh,[†] Emilie Durieu,[†] Benoît Villiers, Céline Bruyère, Thu Lan Nguyen, Xavier Fant, Kwang H. Ahn, Leepakshi Khurana, Emmanuel Deau, Mattias F. Lindberg, Elodie Sévère, Frédéric Miege, Didier Roche, Emmanuelle Limanton, Jean-Martial L'Helgoual'ch, Guillaume Burgy, Solène Guiheneuf, Yann Herault, Debra A. Kendall, François Carreaux, Jean-Pierre Bazureau, and Laurent Meijer*

Cite This: *J. Med. Chem.* 2022, 65, 1396–1417

Read Online

ACCESS | Metrics & More | Article Recommendations | Supporting Information

ABSTRACT: The protein kinase DYRK1A is involved in Alzheimer's disease, Down syndrome, diabetes, viral infections, and leukemia. Leucettines, a family of 2-aminoimidazolin-4-ones derived from the marine sponge alkaloid Leucettamine B, have been developed as pharmacological inhibitors of DYRKs (dual specificity, tyrosine phosphorylation regulated kinases) and CLKs (cdc2-like kinases). We report here on the synthesis and structure–activity relationship (SAR) of 68 Leucettines. Leucettines were tested on 11 purified kinases and in 5 cellular assays: (1) CLK1 pre-mRNA splicing, (2) Threonine-212-Tau phosphorylation, (3) glutamate-induced cell death, (4) autophagy and (5) antagonism of ligand-activated cannabinoid receptor CB1. The Leucettine SAR observed for DYRK1A is essentially identical for CLK1, CLK4, DYRK1B, and DYRK2. DYRK3 and CLK3 are less sensitive to Leucettines. In contrast, the cellular SAR highlights correlations between inhibition of specific kinase targets and some but not all cellular effects. Leucettines deserve further development as potential therapeutics against various diseases on the basis of their molecular targets and cellular effects.

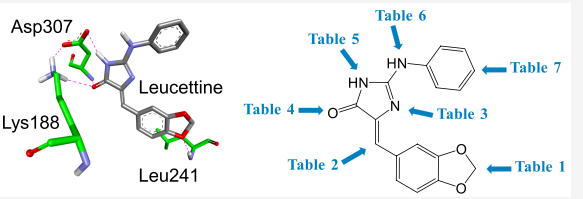

INTRODUCTION

The human kinome comprises 538 protein kinases.[1−4] This wide class of enzymes catalyzes the phosphorylation of serine, threonine, and tyrosine residues in enzymatic and structural proteins. Protein phosphorylation is probably the most frequent post-translational mechanism underlying intracellular regulation. As phosphorylation is frequently deregulated in human diseases, modulation of protein kinases by pharmacological inhibitors (antibodies and low molecular weight molecules) has become a prime therapeutic target approach in the pharmaceutical industry.[5−10] Over 900 000 articles on kinases and phosphorylation have been published, and more than 5000 crystal structures of kinases (with or without inhibitors) have been solved. Almost 19 000 inhibitors have been described with activities against 266 different kinases. Most inhibitors target the ATP-binding site, and most aim at the treatment of cancers. Many kinases have not yet been investigated as therapeutic targets. More than 260 protein kinase inhibitory molecules are in clinical study against various human pathologies.[3] As of February 2021, 62 kinase inhibitors have been approved and are currently marketed.[10] Most of these are tyrosine kinase inhibitors developed for the treatment of cancer.

The CMGC families of DYRKs (dual specificity, tyrosine phosphorylation regulated kinases)[11−16] and CLKs (cdc2-like kinases)[16−20] are considered as potentially important therapeutic targets, especially in the central nervous system area (reviews in refs 13, 15, 16). The DYRKs family comprises five members: DYRK1A, 1B, 2, 3, 4. The CLKs family comprises four members: CLK1, 2, 3, 4. DYRK1A is the most studied DYRK. The *Dyrk1A* gene is located on chromosome 21q22.2, in a region known as the "Down syndrome critical region" (DSCR), responsible for most of the Down syndrome (DS) associated cognitive deficits. There is strong evidence that the mere 1.5-fold increase in DYRK1A expression and activity in DS is associated with some of the most severe aspects of the DS phenotype.[14,15,21−27] Other intellectual and developmental disabilities, including autism spectrum disorders and mental retardation disease 7 (MRD7), are associated with *Dyrk1A* gene mutations or deletions.[28,29] There is also evidence for the

Special Issue: New Horizons in Drug Discovery - Understanding and Advancing Kinase Inhibitors

Received: June 26, 2021
Published: December 20, 2021

https://doi.org/10.1021/acs.jmedchem.1c01141
J. Med. Chem. 2022, 65, 1396–1417

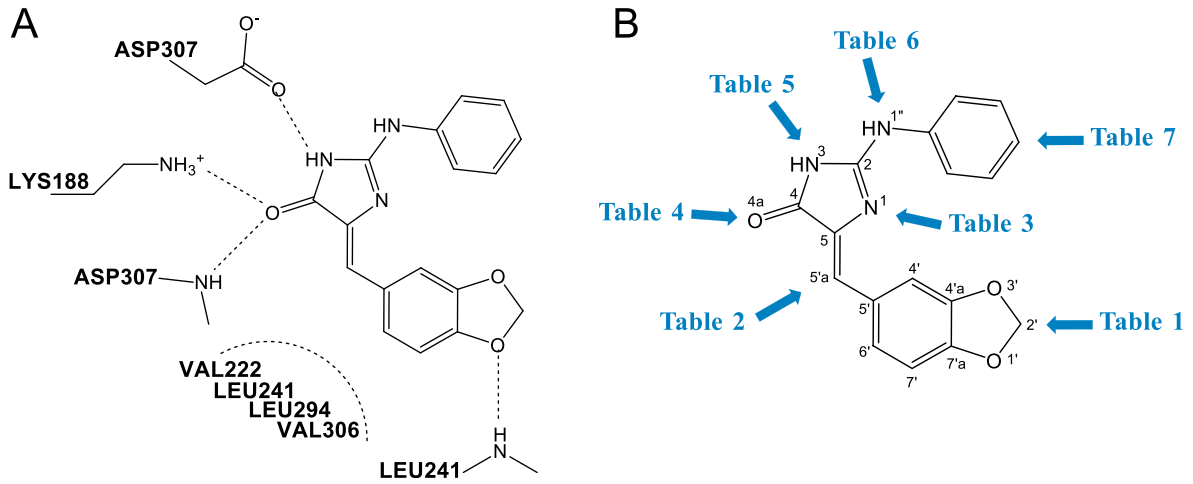

Figure 1. (A) Interactions of Leucettine **L41** with DYRK1A as identified by resolution of a cocrystal structure (PDB: 4AZE). Hydrogen bonds are represented by straight dotted lines. Circled dotted line indicates hydrophobic interactions. (B) Numbering of Leucettine **L41** atoms and structure−activity relationship. Arrows link tables of results corresponding to different interrogated areas of the Leucettine structure.

involvement of DYRK1A in Alzheimer's disease (AD).[30−39] DYRK1A may also be involved in Parkinson's disease (PD),[40,41] where it was recently identified as one of the risk factors.[42] Recent studies[43−52] have shown that DYRK1A inhibition promotes the proliferation of pancreatic β cells, which could have major implications in diabetes. Inhibition of DYRK1A may be useful for the treatment of knee osteoarthritis,[53,54] tendinopathy,[55] various viral infections,[56−60] acute lymphoblastic leukemia (ALL)[61,62] and acute megakaryoblastic leukemia (AMKL),[63] and various cancers (review in ref 64) such as glioblastoma[65] and pancreatic cancer.[66−68]

These reasons have led researchers to screen for, optimize, and characterize pharmacological inhibitors of DYRKs/CLKs (reviews in refs 33, 36, 52, 69). Pharmacological inhibition of DYRK1A has been shown to correct cognitive deficits in a wide variety of animal models of DS and AD.[25,34−39,70−75] Among the first inhibitors, we have extensively investigated Leucettines, a family of inhibitors derived from the natural product Leucettamine B produced by the marine calcareous sponge *Leucetta microraphis*.[76−80] Extensive studies of this class of molecules showed that Leucettines inhibit DYRKs and CLKs but also interact with CK2 (casein kinase 2), Pim1, glycogen synthase kinase-3 (GSK-3), and the lipid kinase PIKfyve.[25,72,81−84]

In this Article, we have characterized the structure−activity relationship (SAR) of a series of 68 Leucettines selected, among >500 synthesized Leucettines, on the basis of substitution diversity and coverage around the central scaffold. We investigated the effects of Leucettines on the catalytic activity of 11 purified kinases, on CLK1 splicing in cultured cells, on Tau phosphorylation at Thr212, on protection against glutamate-induced cell death, on induction of cellular autophagy, and on ligand-activated cannabinoid receptor CB1. Altogether, the results provide clues to understand the interaction of Leucettines with various targets (especially CLK1, CLK4, DYRK1A, DYRK1B, and DYRK2) and suggest molecular mechanisms of action involved in the various cellular effects triggered by Leucettines. They also provide directions for further optimization of this family of kinase inhibitors. Finally, they suggest that some Leucettines favorably combine several molecular and cellular effects which support their development for the treatment of various clinical indications.

RESULTS AND DISCUSSION

Chemical Synthesis of Leucettines. Inspired by the natural product Leucettamine B (**L0**), we have designed and synthesized a wide series of analogues and derivatives of this 2-aminoimidazolone scaffold, collectively called Leucettines. The first series (41 compounds, **L1**−**L41**) has been described previously,[81] among which **L41** was the most thoroughly investigated in terms of selectivity and biological actions.[25,39,72,81−84] We here present a selection from the chemical library of more than 500 Leucettines which have been synthesized.

In order to evaluate the importance of functional groups, we envisaged different strategies to modify the structural skeleton and substituents of **L41** in a targeted manner and at diverse positions, based on the DYRK1A/**L41** cocrystal structure[81] (Figure 1A), with the aim of understanding the SAR in the Leucettines family of kinase inhibitors (Figure 1B).

A first series of analogues **L42**−**L57** (Tables 1 and 2) was prepared with a well-defined stereochemistry as described in Scheme 1, in which the diversity is brought about via a condensation reaction using a large variety of aldehydes. Reaction with acetophenone also led to the desired product but with a more moderate yield (58%) compared to aldehydes due to lower reactivity of ketones. The stereochemistry of condensation products was exclusively *Z* except for Leucettine **L56** which was a mixture of *Z*/*E* isomers (80/20).

Based on the replacement of the imidazolone ring by another five-membered azaheterocyclic system, different Leucettine analogues were prepared according to Schemes 2 and 3. 1,3-Thiazol-4-one derivative **L58** was synthesized from commercially available *N*-phenylthiourea. After ring closure with ethyl bromoacetate, compound **4** underwent a condensation reaction with piperonal under microwave irradiation, affording the desired product **L58** in two steps with an overall 22% yield (Scheme 2). The strategy used for the synthesis of 1,3-oxazolin-5-one derivative **L65** was directly inspired from Molina et al.'s work on the intramolecular addition of an ester group on a carboiimide moiety.[85] The synthesis started with the preparation of methylazido acetate **8** using a method similar to that described in the literature (Scheme 3).[86] Condensation with piperonal provided the corresponding vinyl azide **9** as reported.[87] Following the reaction with triphenyl-

https://doi.org/10.1021/acs.jmedchem.1c01141
J. Med. Chem. 2022, 65, 1396−1417

Table 1. Biological Effects of 15 Leucettines[a]

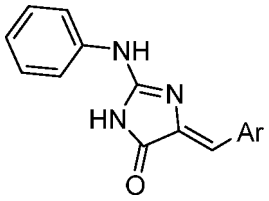

L	Ar	CLK1	CLK2	CLK3	CLK4	DYRK1A	DYRK1B	DYRK2	DYRK3	GSK3	CK2	PIM1	HT22 surival	HT22 & Glutamate	Autophagy	mRNA splicing	P-T212 Tau	CB1
L41	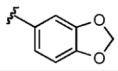	0.023	0.13	1.2	0.023	0.024	0.062	0.014	0.23	0.6	0.51	1.2	>20	6.05	11.6	8.18	-77.2	96.8 0.314
L42	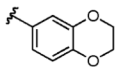	0.13	0.88	2.4	0.14	0.076	0.25	0.092	0.42	2	0.97	1	- (20)	10.0	6.6	3.14	-83.4	96.3
L43	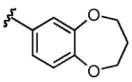	>10	-	-	>10	7.4	>10	>10	-	-	-	>10	- (20)	12.5	5.6	0.15	-67.2	89.3 0.890
L44	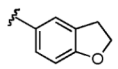	0.022	0.12	1.2	0.019	0.032	0.088	0.041	0.24	>10	1.1	3.2	- (20)	7.00	10.2	8.20	-75.2	96.4
L45	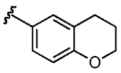	0.12	1.8	⩾10	0.14	0.12	0.36	0.12	0.42	>10	2.2	1.2	>20	3.50	4.8	0.75	-59.8	94.0
L46	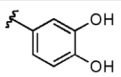	0.21	1.5	2.3	0.13	0.15	0.32	0.27	1.2	1.2	1.5	0.84	- (20)	3.30	10.1	2.69	-74.0	-22.3
L47	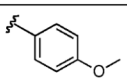	0.34	>10	-	0.28	0.17	0.55	0.22	2.1	-	2.1	⩾10	>20	5.30	5.8	0.42	-66.3	92.2
L48	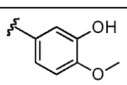	4.3	⩾10	-	4	2	2.8	2.1	2.4	-	>10	1.9	- (20)	5.57	6.5	0.10	-49.4	46.8
L49	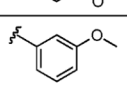	≥10	>10	-	5	>10	-	>10	-	-	-	1.3	>20	7.20	5.7	0.41	-35.1	71.9
L50	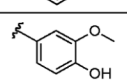	0.021	0.14	0.61	0.023	0.07	0.062	0.033	0.12	1.1	0.62	0.18	>20	1.28	11.7	8.64	-62.4	1.6 4.703
L51	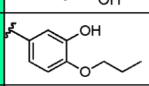	-	-	-	-	-	-	-	-	-	-	-	- (20)	2.45	7.6	0.38	-8.0	54.3
L52		-	-	-	-	-	-	-	-	-	-	-	- (20)	7.20	7.7	0.34	-52.2	44.6
L53	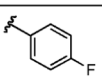	3.2	>10	>10	2.8	9.5	>10	-	-	-	-	>10	- (20)	2.85	(20.2) T	0.19	Inact.	78
L54	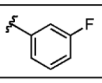	-	-	-	-	>10	-	-	-	-	-	3.2	>20	3.50	5.9	0.08	-44.2	79.5 0.916
L55	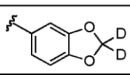	0.04	0.17	0.5	0.029	0.02	0.063	0.035	0.4	0.75	1.6	2.1	- (20)	4.90	7.3	7.71	-76.9	92.7

[a]Compounds were tested at various concentrations on each kinase as described in the Experimental Section. IC_{50} values are reported in μM. −, inactive at the highest concentration tested (10 μM); > 10, inhibitory but IC_{50} > 10 μM. Compounds were also tested (1) for their effects on cell survival (MTS assay, IC_{50} values in μM), (2) for their ability to prevent glutamate (10 mM)-induced HT22 cell death (EC_{50} values in μM), (3) for their ability to induce autophagy in U-2 OS cells (values indicated are averaged number of LC3 foci/cell (triplicates) measured after a 4 h treatment of U-2 OS cells with 10 μM Leucettine; the averaged numbers of LC3 foci/cell were 5.3 ± 0.8 (n = 16 measurements), 10.33 ± 1.37 (n = 16) and 11.64 ± 2.02 (n = 17) for DMSO (negative control), rapamycin and Leucettine **L41** (positive controls), respectively), (4) for their ability to modify the splicing of CLK1 pre-mRNA in HT22 cells (the values indicated for splicing are averaged ΔCt values (triplicates) measured after a 4 h treatment of HT22 cells with 10 μM Leucettine; the ΔCt average from 21 measurements was 0.39 ± 0.25 for DMSO (negative control) and 8.18 ± 0.89 for Leucettine **L41** (positive control)), (5) for their ability to inhibit Tau phosphorylation on Thr212 (values indicate the level of Thr212-Tau phosphorylation compared to vehicle treated cells (100%)), and (6) for their ability to antagonize activation of the cannabinoid receptor CB1 by CP-55940 (last column on the right, DiscoveRx arrestin assay, upper numbers in black indicate % of antagonism for compound tested at 10 μM, while numbers below are IC_{50} values (in μM) calculated from dose−response curves), as described in the Experimental Section.

https://doi.org/10.1021/acs.jmedchem.1c01141
J. Med. Chem. 2022, 65, 1396−1417

Table 2. Biological Effects of 3 Leucettines Evaluated on 11 Purified Protein Kinases, HT22 Cell Survival, Glutamate-Induced HT22 Cell Death, Autophagy in U-2 OS cells, CLK1 mRNA Splicing, Phosphorylation of Tau on Thr212, and Inhibition of CB1[a]

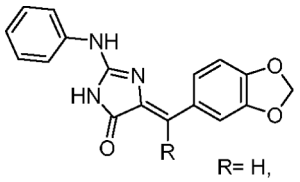

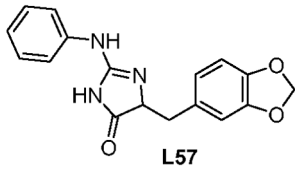

L	CLK1	CLK2	CLK3	CLK4	DYRK1A	DYRK1B	DYRK2	DYRK3	GSK3	CK2	PIM1	HT22 survival	HT22 & Glutamate	Autophagy	mRNA splicing	P-T212 Tau	CB1
L41	0.023	0.13	1.2	0.023	0.024	0.062	0.014	0.23	0.6	0.51	1.2	>20	6.05	11.6	8.18	-77.2	96.8 0.314
L56	≥10	>10	>10	5.9	8.5	>10	1.6	-	-	-	-	>20	- (20)	5.8	0.38	-25.9	-42.1
L57	6.27	>10	>10	5.6	5.1	>10	>10	>10	>10	nt	nt	>20	nt	nt	nt	nt	nt

[a]See footnote of Table 1.

Scheme 1. General Procedure for the Introduction of Substituents at Position 5 of the Imidazolone Ring (Tables 1 and 2)[a]

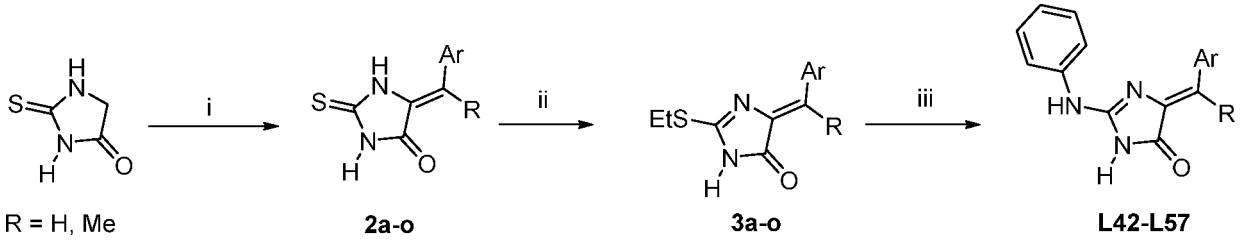

[a]Reagents and conditions: (i) Method A: ArCH = *N*-Pr, CH_3CN, 80 °C, 14 h; Method B: aldehyde or ketone, AcOH, AcONa, $\mu\omega$, 140 °C, 20 min. (ii) EtI, K_2CO_3, DMF, 60 °C, 14 h, 14−95%. (iii) $PhNH_2$, $\mu\omega$, 140−160 °C, 30 min, 15−75%.

Scheme 2. Synthesis of L58, a Leucettine Analogue Containing a 1,3-Thiazol-4-one Scaffold (Table 3)[a]

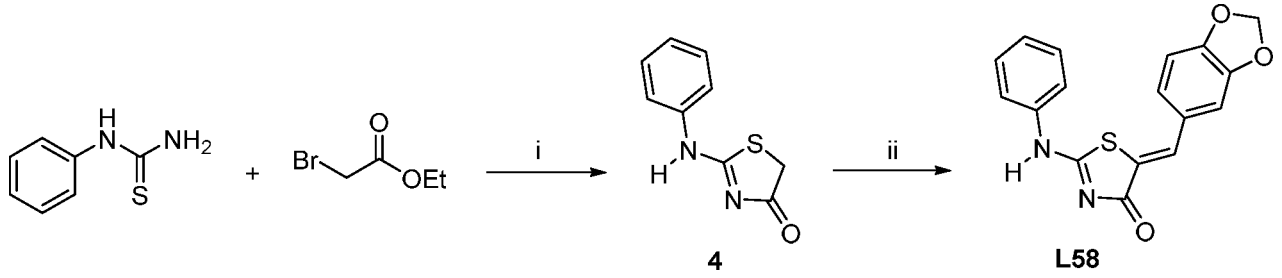

[a]Reagents and conditions: (i) EtOH, 55 °C, 3.5 h, 64%; (ii) $PhNH_2$, $\mu\omega$ (Explorer 24 CEM reactor), 150 °C, 20 min, 34%.

phosphine, treatment of iminophosphorane **10** with phenyl isocyanate led to the formation of the corresponding transient carbodiimide, which undergoes a cyclization step in the presence of tetrabutylammonium fluoride (TBAF) to afford **L65** with a 41% yield.

Finally, we explored the synthesis of Leucettines with different substituents at the 2-amino position (*N1"*) of the imidazol-4-one scaffold as shown in Scheme 4. *S*-Alkyl products (**L59**, **L62**, **14**) were obtained by alkylation of the corresponding (*Z*)-thiohydantoin with the appropriate halogenated reagent. N-Substituted analogues were prepared by displacement of the SEt group under microwave irradiation conditions with a large variety of primary and secondary aromatic amines. The yield of this last step was highly dependent on the steric hindrance of the amine used. For example, while a 34% yield was obtained with 2,5-dimethylani-

https://doi.org/10.1021/acs.jmedchem.1c01141
J. Med. Chem. 2022, 65, 1396−1417

Scheme 3. Synthesis of L65, a Leucettine Analogue Containing a 1,3-Oxazol-4-one Scaffold (Table 5)[a]

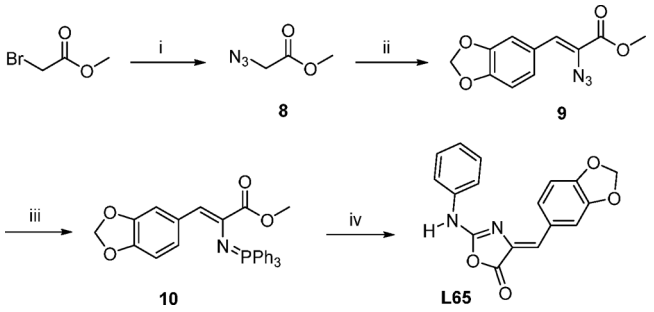

[a]Reagents and conditions: (i) NaN_3, $\mu\omega$ (Monowave 300 Anton Paar reactor), 160 °C, 1 h, 56%; (ii) piperonal, MeONa, −20 °C, 3 h, 21%; (iii) PPh_3, rt, 12 h; (iv) (a) Phenylisocyanate, THF, 0 °C, 2 h (b) TBAF, THF, rt, 2 h, 41%.

line, a 67% yield was reached with 3,4-dimethylaniline. A strong decrease in the yield was also observed when aniline was replaced by *N*-methylaniline. Introduction of a primary alkylamine can be carried out after concomitant oxidation of (*Z*)-thiohydantoin **12** using *tert*-butyl hydroperoxide (TBHP). Using methylamine, **L64** was obtained with a 68% yield.

Compounds described in this Article were typically precipitated by a solvent such as ethanol or ether and were either sufficiently pure for biological tests or purified by silica gel chromatography (purity was determined by high resolution mass spectroscopy and microanalysis and was >95% in all cases). Beside **L56**, all compounds were obtained in a stereospecific manner as determined on the basis of $^{13}C/^{1}H$ long-range coupling constants measured in gradient heteronuclear single quantum multiple bond correlation (gHSQMBC) experiments.

Structure−Activity Relationship of Leucettines. *(1) Purified Protein Kinase Targets.* Based on the crystal structures of Leucettine L41 with various kinases,[81,82] we selected a series of 68 Leucettines (55 new + 13 Leucettines described in ref 81) covering modulations on various domains of the Leucettine scaffold (Figure 1) (Tables 1−7). These modifications were chosen with the aim of "interrogating" the importance of each Leucettine domain/atom in its interaction with reported Leucettine targets. Eleven kinases were expressed, affinity purified, and assayed in the presence of each of the 68 Leucettines: CLK1, 2, 3, 4; DYRK1A, 1B, 2, 3; GSK-

Scheme 4. General Procedure for the Synthesis of Leucettines Substituted at the C2-Amino Position of the Imidazolone Platform (Tables 1, 6, 7)[a]

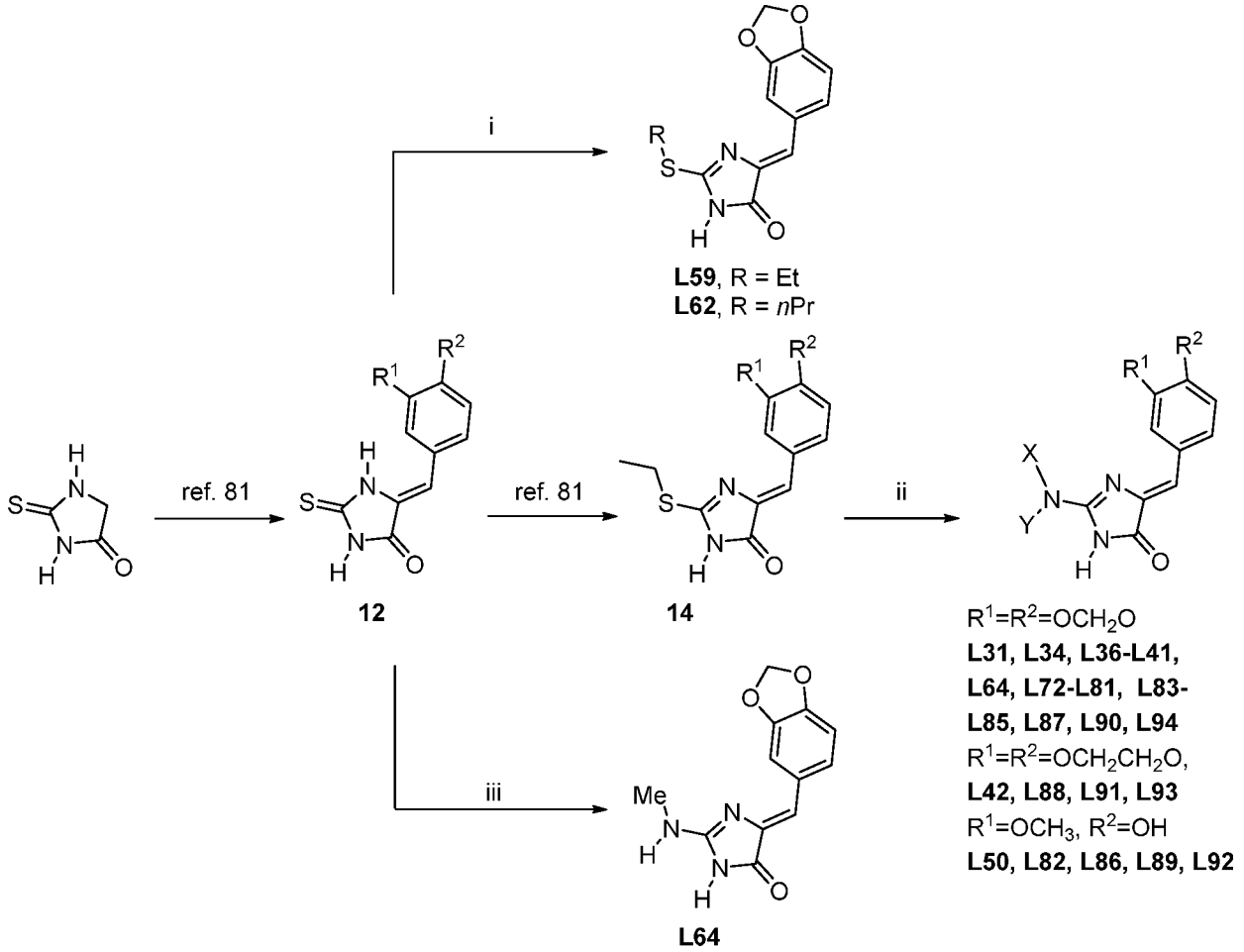

[a]Reagents and conditions: (i) RI, K_2CO_3, CH_3CN, 66 °C, 14 h, 54% (**13a**), 94% (**13b**); (ii) XYNH, $\mu\omega$, 160−205 °C, 30 min, 9−75%; (iii) $MeNH_2$, TBHP, MeOH, rt, 24 h, 68%.

https://doi.org/10.1021/acs.jmedchem.1c01141
J. Med. Chem. 2022, 65, 1396−1417

3α/β; CK2; PIM1. Compounds were first tested at a 10 μM final concentration, and those displaying more than 50% inhibition at this concentration were further tested in dose−response curves to allow the determination of IC_{50} values, which are reported in Tables 1−7. Results are summarized in Figure 2. All assays were run at least twice in triplicates.

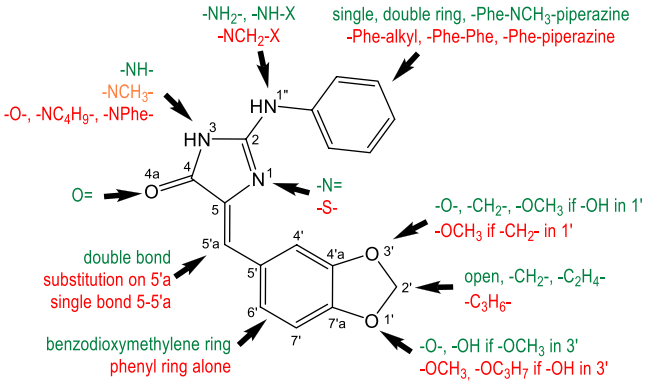

Figure 2. Summary of SAR results in terms of kinase inhibition. Green, orange, red: favorable, acceptable, unfavorable modifications, respectively.

Table 1 investigates the relationship between the benzodioxole ring system and the kinase inhibition potency with special focus on DYRK1A (Figure 1). Results clearly show that a benzodioxole ring is optimal, that a benzodioxane ring leads to a modest reduction of the inhibitory activity on all kinases, and that a benzodioxepine ring leads to complete inactivation of the inhibitory activity (compare **L41**, **L42**, and **L43**, or **L44** and **L45**). This suggests that this ring system has to be flat to keep its affinity for DYRK1A. Alternatively, an open ring is equally potent (compare **L41** with **L50**) as long as there is an oxygen in *para* (compare **L41**, **L47**, **L50** with **L49**, **L52**−**L54**), preferably a hydroxy than a methoxy group (compare **L48** with **L50**). Results also show that a methoxy in the *para*-position of the aromatic ring is much preferable than that in the *meta*-position (compare **L47** and **L49**). Comparison of compounds **L41** with **L44** and **L42** with **L45** shows that the presence of an oxygen atom in 3′ is not required. All these results fit with the H-bond between an oxygen in 1′ and the backbone nitrogen of Leu241 in DYRK1A (Figure 1A). Except for **L43**, **L46**, and **L48** that might suffer from a suboptimal orientation of the H-bond interaction, the DYRK1A potency is directly related to the electronegativity of this oxygen in the *para*-position (Supporting Information (SI) Figure S3). A butoxy group in the same position (**L51**), the lack of a 1′ substituent (**L52**), or a fluorine in 1′ (**L53**) or 3′ (**L54**) prevent kinase inhibitory activity. Deuterated benzodioxole (**L55**) and **L41** display similar activities.

Table 2 investigates the importance of the carbon (position 5′a) linking the benzodioxole ring system and the 2-aminoimidazolin-4-one platform structure (Figure 1). Substitution by a methyl group at this site (**L56**) or reduction of the double bond (**L57**) strongly reduces the kinase inhibitory activities, suggesting that very little steric modification is possible at this site. The 5−5′a double is a potential site for conjugation. We have tested this possibility with **L41** and **L92** (50 μM) by incubation (60 min) with pooled human liver microsomes (1 mg/mL) and glutathione (GSH) (1:1 ratio of unlabeled GSH to $^{13}C_2$,^{15}N-GSH) with and without NADPH. Supernatants are analyzed by LC-MS/MS. A GSH + reduction + demethylation metabolite was identified in the case of **L41**. This metabolite represented 0.12% of the total product. No metabolites were identified with **L92**. Conjugation occurred in the absence of NADPH, suggesting a chemical rather than metabolic conjugation. GSH adduct is thus possible but to a very limited level.

Table 3. Biological Effects of 4 Leucettines Evaluated on 11 Purified Protein Kinases, HT22 Cell Survival, Glutamate-Induced HT22 Cell Death, Autophagy in U-2 OS Cells, CLK1 mRNA Splicing, Phosphorylation of Tau on Thr212, and Inhibition of CB1[a]

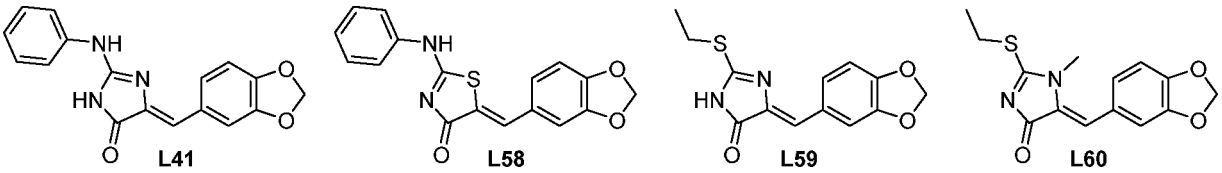

L	CLK1	CLK2	CLK3	CLK4	DYRK1A	DYRK1B	DYRK2	DYRK3	GSK3	CK2	PIM1	HT22 survival	HT22 & Glutamate	Autophagy	mRNA splicing	P-T212 Tau	CB1
L41	0.023	0.13	1.2	0.023	0.024	0.062	0.014	0.23	0.6	0.51	1.2	>20	6.05	11.6	8.18	-77.2	96.8 0.314
L58	0.8	5	>10	0.43	1.2	10	0.61	>10	-	2.5	>10	>20	- (20)	5.9	- 0.09	-68.1	-5.9
L59	0.029	0.12	1.4	0.023	0.033	0.072	0.032	0.16	0.9	0.6	0.34	>20	- (20)	5.5	0.57	-60.6	-7.5
L60	-	-	-	-	-	-	-	-	-	-	-	- (20)	- (20)	6.5	0.23	Inact.	-10.7

[a]See footnote of Table 1.

https://doi.org/10.1021/acs.jmedchem.1c01141
J. Med. Chem. 2022, 65, 1396−1417

Table 4. Biological Effects of 3 Leucettines Evaluated on 11 Purified Protein Kinases, HT22 Cell Survival, Glutamate-Induced HT22 Cell Death, Autophagy in U-2 OS Cells, CLK1 mRNA Splicing, Phosphorylation of Tau on Thr212, and Inhibition of CB1[a]

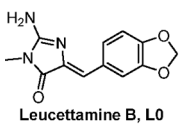

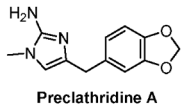

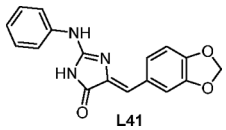

L	CLK1	CLK2	CLK3	CLK4	DYRK1A	DYRK1B	DYRK2	DYRK3	GSK3	CK2	PIM1	HT22 surival	HT22 & Glutamate	Autophagy	mRNA splicing	P-T212 Tau	CB1
L0 (Leucettamine B)	0.14	0.94	6	0.12	0.22	1.6	0.43	1.3	5	-	>10	- (20)	- (20)	4.3	1.14	Inact.	9.5 >10
Preclathridine A	3.2	>10	>10	3	>10	-	>10	>10	-	-	-	- (20)	- (20)	5.3	0.38	-29.6	8.9
L41	0.023	0.13	1.2	0.023	0.024	0.062	0.014	0.23	0.6	0.51	1.2	>20	6.05	11.6	8.18	-77.2	96.8 0.314

[a]See footnote of Table 1.

Table 3 investigates the importance of *N*1 in the imidazolone ring structure (Figure 1). Replacement of this atom by sulfur strongly reduces the inhibitory potency (compare **L58** with **L41**). Methylation at *N*1 blocks *N*3 in a stable double bond and this completely abolishes the kinase inhibitory activity (compare **L59** and **L60**).

Table 4 investigates the importance of the carbonyl group (position 4) in the 2-aminoimidazolin-4-one ring structure (Figure 1). Comparison of Leucettamine B (**L0**) and preclathridine A, which only differ by this carbonyl group, immediately reveals that this is an essential group. Cocrystal structures with DYRK1A confirm key H-bonds between the carbonyl moiety of Leucettines and Lys188 and Asp307 (Figure 1A).

Table 5 investigates the importance of substituents at the *N*3 position in the 2-aminoimidazolin-4-one platform structure (Figure 1). N-Methylation partly reduces the kinase inhibition properties (compare **L41** with **L21**, **L64** with **L0** and **L3** with **L31**), though much less than methylation of *N*1 (**L60**) (Table 3). This effect of *N*3 methylation is also seen in the molecules where *N*1" is replaced by an alkylated sulfur (compare **L59** with **L61**, **L62** with **L63**) or left as a primary amine (compare **L64** and **L0**). Larger substituents at *N*3 lead to complete lack of kinase inhibitory activity (**L32**, **L33**). Replacement of *N*3 by an oxygen atom completely inactivates the compound (compare **L65** with **L41**). These results fit with the observation that *N*3 acts as a H-bond donor with the carbonyl moiety of Asp307 (Figure 1A). The residual activity when the *N*3 H-bond donor possibility is lacking (**L0**, **L21**, **L31**, **L61**, **L63**) may either come from a shift of this H-bond to the exocyclic nitrogen (*N*1") and the ability of the kinase to allow the presence of a methyl but not a larger size substituent on *N*3, or to the fact that H-bonding between *N*3 and Asp307 may not be crucial.

Table 6 investigates the importance of the exocyclic amine (*N*1") on position 2 (Figure 1). A single substitution on *N*1" appears to be better than two substitutions (compare **L41** with **L67**, **L68**, **L69**, **L70**). Although a primary amine leads to quite an active compound (**L64**), a single substitution of *N*1" with a methyl (**L66**) or a propyl (**L31**) reduces the kinase inhibitory activity effects. However, when the size of the substituent is increased (**L41**, phenyl), the compound regains potent activity (compare **L64** with **L41**). Replacement of the nitrogen by a sulfur leads to slightly active molecules (compare **L66** with **L71**, **L31** with **L62**). Increasing the size of the alkyl substituent on sulfur leads to an increased inhibitory potency (compare **L71** with **L62**).

Table 7 investigates the importance of substituents on the *N*1" position (Figure 1). Compared to the *N*1" unsubstituted primary amine (**L64**), most but not all monocyclic (**L41**, **L36**−**38**, **L72**−**L79**) or bicyclic (**L39**, **L40**, **L83**−**L94**) substitutions maintain or even enhance the kinase inhibitory potency. When the phenyl of **L41** is substituted with a piperazine, kinase inhibition is reduced (compare **L41** with **L87**, and **L42** (Table 1) with **L88**, **L50** (Table 1) with **L89**). A mere N-methylation of the piperazine moiety greatly increases the kinase inhibitory potency (compare **L87** with **L90**, **L88** with **L91**, and **L89** with **L92**). Clearly, a rather large hydrophobic pocket surrounding the phenyl of the original **L41** deserves further chemical exploration.

At the start of this work, we were hoping to find subclasses of Leucettines that would have stronger affinity for specific CLKs or DYRKs. Unfortunately, this was not the case and all compounds active on DYRK1A (our primary target of interest in the context of DS and AD) were found to be roughly equipotent on CLK1, CLK4, DYRK1B, and DYRK2. CLK2 and DYRK3 were slightly less sensitive, and CLK3 even less. The amino acids involved in binding of **L41** to DYRK1A (Lys188, Val222, Leu241, Leu 294, Val306, Asp307) (Figure 1A) are fully conserved in CLK1, CLK4, and DYRK1B. In DYRK2 and DYRK3, the two Valines are replaced by Isoleucines. In CLK3, Val306 is replaced by an Alanine (SI, Table S3). The SAR results described for DYRK1A are essentially identical for CLK1, CLK4, DYRK1B, and DYRK2. These SAR results in terms of kinase inhibition are summarized in Figure 2. The best potencies obtained with compounds **L90** and **L91** can be rationalized by docking experiments showing an additional H-bond interaction between the piperazine residue of these two compounds and the Asp247 amino acid residues of DYRK1A (Figure 3).

https://doi.org/10.1021/acs.jmedchem.1c01141
J. Med. Chem. 2022, 65, 1396−1417

Table 5. Biological Effects of 13 Leucettines Evaluated on 11 Purified Protein Kinases, HT22 Cell Survival, Glutamate-Induced HT22 Cell Death, Autophagy in U-2 OS Cells, CLK1 mRNA Splicing, Phosphorylation of Tau on Thr212, and Inhibition of CB1[a]

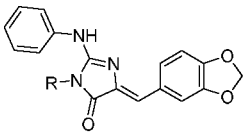

R = H, **L41**
R = Me, **L21**

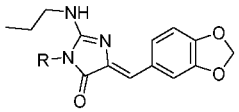

R = H, **L31**
R = CH_3, **L3**
R = C_3H_7, **L32**
R = Ph, **L33**

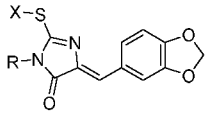

R = H, X = C_2H_5, **L59**
R = Me, X = C_2H_5, **L61**
R = H, X = C_3H_7, **L62**
R = Me, X = C_3H_7, **L63**

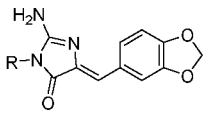

R = H, **L64**
R = CH_3, **L0**

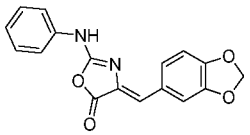

L65

L	CLK1	CLK2	CLK3	CLK4	DYRK1A	DYRK1B	DYRK2	DYRK3	GSK3	CK2	PIM1	HT22 survival	HT22 & Glutamate	Autophagy	mRNA splicing	P-T212 Tau	CB1
L41	0.023	0.13	1.2	0.023	0.024	0.062	0.014	0.23	0.6	0.51	1.2	- (20)	6.05	11.6	8.18	-77.2	96.8 0.314
L21	0.14	0.5	1.4	0.11	0.093	3.2	0.08	0.87	0.75	>10	≥10	- (20)	14.00	7.9	4.42	-40.4	-5.5
L31	0.07	0.55	3	0.061	0.12	0.31	0.1	0.65	4.1	1.4	1.2	>20	- (20)	5.1	5.11	-47.2	-14.8
L3	0.11	0.56	2.5	0.12	0.46	0.55	0.095	1.2	1.4	>10	3.2	- (20)	>20	6.8	3.72	-47.2	-15.8
L32	3	≥10	>10	2.3	>10	>10	>10	>10	>10	-	-	- (20)	- (20)	5.0	-0.32	-1.5	-13.4
L33	2	2.5	9.5	1.2	>10	>10	7.2	7	>10	-	-	>20	- (20)	4.7	-0.05	-38.8	-17.9
L59	0.029	0.12	1.4	0.023	0.033	0.072	0.2	0.16	0.9	0.6	0.34	- (20)	- (20)	5.5	0.57	-60.6	-7.5
L61	0.12	0.42	2.1	0.11	0.24	0.98	0.34	0.3	1.1	>10	2.1	- (20)	- (20)	6.8	-0.99	-20.4	-0.7
L62	0.034	0.11	3.1	0.027	0.04	0.09	0.037	0.51	1.4	1.7	0.95	>20	- (20)	7.3	2.48	-2.4	-2.6
L63	0.064	0.32	>10	0.022	0.34	0.62	0.33	0.62	2	>10	2	- (20)	- (20)	6.2	-1.36	-16.1	37.2
L64	0.041	0.18	0.95	0.037	0.035	0.19	0.032	0.24	2.1	0.93	0.32	>20	- (20)	5.0	3.02	-27.0	-2.2
L65	-	-	-	-	-	-	-	-	-	-	-	- (20)	- (20)	6.2	-0.18	Inact.	-37.5
L0	0.14	0.94	6	0.12	0.22	1.6	0.43	1.3	5	-	>10	- (20)	- (20)	4.3	1.14	Inact.	9.5

[a]See footnote of Table 1.

We also used these SAR results to compare the sensitivity of various DYRKs and CLKs to Leucettines taken as a whole chemical family. Strong correlations were observed when Leucettine IC_{50} values on the different DYRKs and CLKs were plotted against the IC_{50} values toward DYRK1A (Figure S4). IC_{50} values for each kinase were plotted against IC_{50} values for all other kinases, and Rsqr was calculated from the plots (SI Tables S1, S2 and Figure S4). Homology in the catalytic domain sequence of all CLK and DYRK kinases tested was also compared (SI Table S1). Comparative sensitivity of the kinases to Leucettine inhibition directly correlates with comparative homology between the sequence of their kinase domain (Tables S1, S2 and Figure S4).

(2) CLK1 Pre-mRNA Splicing. DYRK1A regulates pre-mRNA splicing by phosphorylating various splicing factors (SRSF6, ASF, SF3b1/SAP155, etc.).[88−97] CLK1, through its action on the phosphorylation of serine/arginine-rich proteins (SRp), is a key regulator of pre-mRNA splicing.[98−100] The

https://doi.org/10.1021/acs.jmedchem.1c01141
J. Med. Chem. 2022, 65, 1396−1417

Table 6. Biological Effects of 10 Leucettines Evaluated on 11 Purified Protein Kinases, HT22 Cell Survival, Glutamate-Induced HT22 Cell Death, Autophagy in U-2 OS Cells, CLK1 mRNA Splicing, Phosphorylation of Tau on Thr212, and Inhibition of CB1[a]

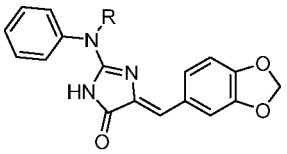

R = H, **L41**
R = Me, **L67**

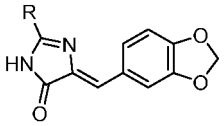

R = NH_2, **L64**
R = NH-alk, **L31, L66**
R = $N(alk)_2$, **L68, L69, L70**
R = S-alk, **L62, L71**

L	R	CLK1	CLK2	CLK3	CLK4	DYRK1A	DYRK1B	DYRK2	DYRK3	GSK3	CK2	PIM1	HT22 surival	HT22 & Glutamate	Autophagy	mRNA splicing	P-T212 Tau	CB1
L41		0.023	0.13	1.2	0.023	0.024	0.062	0.014	0.23	0.6	0.51	1.2	>20	6.05	11.6	8.18	-77.2	96.8 0.314
L67		0.31	1.2	2.6	0.13	0.38	0.68	0.32	1.8	6.2	2.1	2	>20	> 20	4.7	1.16	-40.6	-9.1
L64		0.041	0.18	0.34	0.037	0.035	0.19	0.032	0.24	2.1	0.93	0.32	>20	- (20)	5.0	3.02	-27.0	-2.2
L66	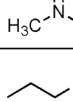	0.14	0.53	1.2	0.094	0.16	0.5	0.13	0.48	6.2	1.8	1.2	>20	- (20)	4.9	1.00	Inact.	-14.7
L31		0.07	0.55	3	0.061	0.12	0.31	0.1	0.65	4.1	1.4	1.2	>20	- (20)	5.1	5.11	-47.2	-14.8
L68		0.6	2.3	3.2	0.38	0.63	2.3	0.93	0.93	6.2	1.2	1.5	- (20)	- (20)	5.0	0.05	-11.0	-59.1 - (10)
L69		0.24	1.3	4.5	0.25	0.13	0.44	0.22	0.53	2.6	0.76	0.88	- (20)	- (20)	6.8	0.68	Inact.	-58.4
L70		0.43	1.5	5.6	0.29	0.44	1.7	0.41	1.9	6.5	1.1	2.4	- (20)	- (20)	6.5	0.63	Inact.	-51
L71		0.073	0.25	2.4	0.08	0.11	0.33	0.08	0.41	1.8	2.2	1.2	- (20)	- (20)	5.9	0.13	-25.4	-23
L62		0.034	0.11	3.1	0.027	0.04	0.09	0.037	0.51	1.4	1.7	0.95	>20	- (20)	7.3	2.48	-2.4	-2.6

[a]See footnote of Table 1.

catalytic activity of CLK1 regulates alternative splicing of CLK1 pre-mRNA itself at the level of exon 4 (Figure 4A). In the presence of active CLK1, there is a roughly equal proportion between the forms including or excluding exon 4. Genetic inactivation or pharmacological inhibition of CLK1 catalytic activity leads to massive inclusion of exon 4.[98−100] We used this as a reporter system to detect CLK1 inhibition in a cellular context using immortalized mouse hippocampal HT22 cells (see also ref 82). Primers were designed to detect the two main splice variants of CLK1 (Figure 4A, B). A preliminary time-course study performed with **L41** showed that a maximal effect on exon 4 inclusion is already reached after 3 h of treatment (data not shown). HT22 cells were next treated for 6 h with 10 μM of each of the 68 Leucettines. Cells were lysed, and total mRNA was purified and reverse-transcribed in 96-well plates. The relative quantity of both splice variants was quantified by qPCR (ΔC_t measurement) using specific primers (Figure 4A, B). Each 96-well qPCR plate contained negative (DMSO, dimethyl sulfoxide) and positive (**L41**) controls. The mean ΔCt of 21 measurements was 0.39 $\pm$ 0.25 for DMSO and 8.18 $\pm$ 0.89 for **L41**, which gives a dynamic range of 21 (8.18/0.39 = 20.97).

Results showed that exon 4 inclusion induced by several Leucettines correlates well with their inhibitory properties toward CLKs and DYRKs (Figure 4C, Tables 1−7). All Leucettines active in this assay were potent inhibitors of both kinase families, but splicing inhibition could not be attributed to a specific CLK or DYRK, suggesting the possible additive effects on several kinases. Structural modifications that lead to inactivation of kinase inhibitory activity abolished the effect on exon 4 inclusion in the CLK1 pre-mRNA, as illustrated in Figure 4C with a selection of Leucettines. A few potent kinase inhibitors (for example, **L59**, **L64**, **L92**) did not affect splicing.

https://doi.org/10.1021/acs.jmedchem.1c01141
J. Med. Chem. 2022, 65, 1396−1417

Table 7. Biological Effects of 32 Leucettines Evaluated on 11 Purified Protein Kinases, HT22 Cell Survival, Glutamate-Induced HT22 Cell Death, Autophagy in U-2 OS Cells, CLK1 mRNA Splicing, Phosphorylation of Tau on Thr212, and Inhibition of CB1[a]

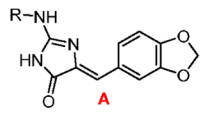

L31, L34, L36-L41, L64, L72-L81, L83, L85, L87, L90, L94

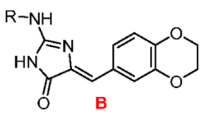

L88, L91

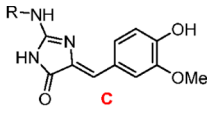

L82, L86, L89, L92

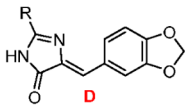

L84

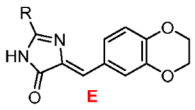

L93

L	Scaffold	R	CLK1	CLK2	CLK3	CLK4	DYRK1A	DYRK1B	DYRK2	DYRK3	GSK3	CK2	PIM1	HT22 surival	HT22 & Glutamate	Autophagy	mRNA splicing	P-T212 Tau	CB1
L64	A	H	0.041	0.18	0.34	0.037	0.035	0.19	0.032	0.24	2.1	0.93	0.32	>20	- (20)	5.0	3.02	-27.0	-2.2
L31	A	Me	0.14	0.53	1.2	0.094	0.16	0.5	0.13	0.48	6.2	1.8	1.2	>20	- (20)	4.9	1.00	Inact.	-14.7
L34	A	Me	0.065	0.38	2.3	0.06	0.14	0.48	0.19	0.47	2.4	0.41	1.2	- (20)	- (20)	5.6	2.64	-6.0	-40.4
L72	A	HN	0.22	0.9	5.3	0.26	0.34	0.65	0.25	0.91	1.3	>10	6.4	- (20)	- (20)	7.4	0.36	Inact.	-43.5
L73	A	N	0.072	0.22	0.51	0.053	0.044	0.2	0.033	0.31	1.7	0.13	0.48	>20	> 20	5.5	6.60	-47.1	-18.3
L41	A		0.023	0.13	1.2	0.023	0.024	0.062	0.014	0.23	0.6	0.51	1.2	>20	6.05	11.6	8.18	-77.2	96.8 0.314
L74	A	F	0.062	0.26	>10	0.05	0.028	0.1	0.035	0.93	8.8	2.2	9.3	- (20)	3.60	4.9	5.73	-44.3.	76.4
L75	A	F	0.052	0.13	0.56	0.03	0.019	0.035	0.023	0.35	0.56	0.8	1.2	- (20)	5.00	7.5	8.85	-52.9	83.4
L76	A	F HO	0.016	0.12	0.4	0.019	0.012	0.023	0.011	0.17	0.55	0.32	0.61	- (20)	13.00	18.2	9.73	-60.7	-5.6
L37	A	HO	0.022	0.083	0.28	0.018	0.013	0.024	0.011	0.14	0.53	0.14	1.1	>20	9.00	12.0	7.91	-51.1	-25.5 - (10)
L38	A	O	0.14	7.5	>10	0.13	0.11	0.27	0.13	6	>10	>10	>10	- (20)	- (20)	5.9	0.50	-14.3.	50.5
L36	A	Me	0.053	1.0	>10	0.056	0.018	0.053	0.034	0.32	7.3	1.7	3.5	- (20)	3.20	8.4	2.29	-50.4.	90.8
L77	A	Me Me	0.24	1.1	>10	0.14	0.072	0.16	0.075	0.95	1.4	2.4	2.5	- (20)	8.00	5.6	1.21	-18.7	64.6
L78	A	Me Me	0.28	2.2	>10	0.16	0.13	0.52	0.055	1.7	>10	>10	>10	>20	2.70	6.6	4.57	-43.4	51.7
L79	A	Me Me	0.05	0.18	3.5	0.023	0.024	0.092	0.022	0.8	10	1.6	7.7	- (20)	7.00	(26.0)T	6.10	Inact.	10.8

https://doi.org/10.1021/acs.jmedchem.1c01141
J. Med. Chem. 2022, 65, 1396−1417

Table 7. continued

L	Scaffold	R	CLK1	CLK2	CLK3	CLK4	DYRK1A	DYRK1B	DYRK2	DYRK3	GSK3	CK2	PIM1	HT22 surival	HT22 & Glutamate	Autophagy	mRNA splicing	P-T212 Tau	CB1
L80	A	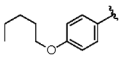	0.85	3.1	>10	0.62	0.71	2.3	0.51	7	>10	1.3	≥10	- (20)	1.14	7.0	0.01	-18.1	37.4
L81	A	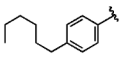	>10	-	-	4.1	>10	>10	9.5	-	-	-	-	- (20)	1.19	6.5	0.03	-39.1	75
L82	C	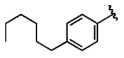	>10	-	-	>10	≥10	≥10	≥10	>10	-	-	>10	>20	0.27	7.6	0.82	-11.8	48.1 2.005
L39	A		0.035	0.13	>10	0.025	0.01	0.04	0.012	0.18	3.4	0.22	8	- (20)	4.90	6.3	6.15	-58.4	76.6
L40	A		0.071	0.21	1.4	0.037	0.03	0.056	0.035	0.33	0.61	0.33	1.5	>20	3.60	4.6	6.14	-74.1	87.3
L83	A	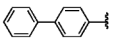	>10	>10	-	5.2	8.1	>10	4.2	-	-	-	-	- (20)	> 20	6.8	0.30	-5.1	36.8
L84	D	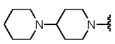	0.92	3.2	>10	1.4	1.1	4.4	1.4	5.2	6.2	>10	7.6	- (20)	- (20)	7.1	0.42	Inact.	-51.1
L85	A	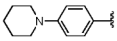	4.2	>10	-	1.5	0.7	2.1	0.23	>10	>10	-	-	- (20)	0.66	11.4	0.28	-16.5	81.7 0.0913
L86	C	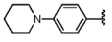	0.75	>10	-	1.2	0.28	0.41	0.41	0.3	>10	-	6.3	- (10)	1.35	10.9	0.33	-47.5	84.1 0.297
L87	A	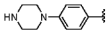	0.42	1.8	9	0.52	0.35	0.95	0.41	1.2	2.4	2.3	6.1	- (20)	0.91	7.3	0.37	Inact.	-47.5
L88	B	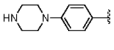	1.1	2.3	>10	0.64	0.53	1.4	0.35	1.1	4.6	3	5.4	- (20)	1.25	7.3	0.41	Inact.	-20
L89	C	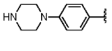	1.2	3.5	>10	1.2	1.3	2.2	2.1	1.5	6.5	-	>10	- (20)	7.00	6.3	0.72	-14.4	-26.8
L90	A	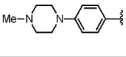	0.023	0.035	0.8	0.016	0.012	0.014	0.05	0.025	0.12	1.2	1.1	- (20)	> 20	(24.9) T	7.48	-67.0	-14.5
L91	B	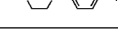	0.017	0.067	1.1	0.019	0.007	0.02	0.008	0.014	0.12	0.45	0.51	>20	12.00	22.0	6.68	-42.1	-1.4
L92	C	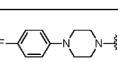	0.012	0.03	0.7	0.012	0.014	0.02	0.015	0.01	0.2	-	0.21	- (20)	> 20	22.0	0.52	-44.4	14.3 - (10)
L93	E	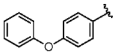	2.1	10	>10	2.3	3.1	≥10	2.2	2.1	8.2	-	9.3	>20	14.00	8.1	0.12	Inact.	16
L94	A		1.8	>10	-	0.76	0.92	4	1.1	-	>10	-	-	- (20)	2.40	4.6	0.18	Inact.	73.5

[a]See footnote of Table 1.

This may be due to either poor cell permeability or interaction with other unidentified cellular targets.

(3) Inhibition of Tau Phosphorylation at Thr212. Phosphorylation of the microtubule binding protein Tau is one of the hallmarks of AD.[101] DYRK1A is one of the kinases that phosphorylates Tau.[31,33,102,103] Using SH-SY5Y-Tau4R, a neuroblastoma cell line overexpressing the full-length form of human Tau,[104] we first tested the effects of **L41** on Tau phosphorylation at different sites, as revealed by several phospho-specific antibodies (Figure 5A). Cells were treated or not with 10 μM **L41** for 6 h, and Tau phosphorylation was estimated by Western blotting. Results revealed that phosphorylation of the Ser202 + Thr205 (AT8 epitope), Thr212, Thr231 (AT180 epitope), Ser262, and to a lower extent Thr181 was reduced by **L41** treatment, especially that of Thr212, a reported phosphorylation site for DYRK1A.[102,103] Thr212 phosphorylation allows the phosphorylation of Thr208 by GSK-3, illustrating the substrate "priming" properties of

https://doi.org/10.1021/acs.jmedchem.1c01141
J. Med. Chem. 2022, 65, 1396−1417

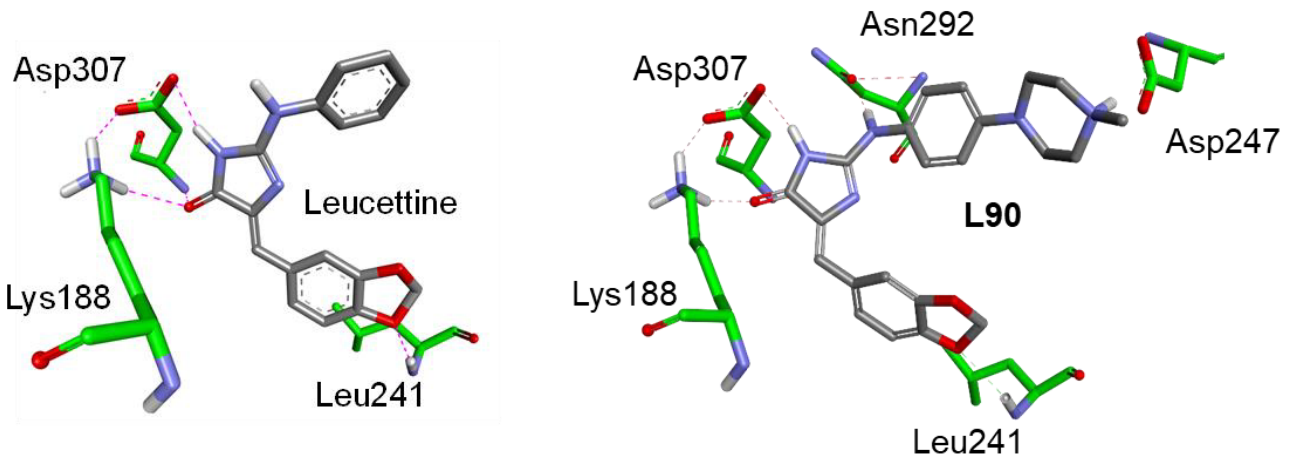

Figure 3. X-ray structure of **L41** compared with the docking pose of **L90** in PDB 4AZE. Ligands are represented as colored by element gray sticks and key amino acid residues of DYRK1A in green sticks. **L90** was scored with a ΔG of interaction of −36.6 KJ, coherent with the experimental value determined (**L90** IC_{50} 12 nM). The slightly higher potency of **L90** compared to **L41** (IC_{50} 24 nM) can result from the additional interactions observed with Asn292 and Asp247 amino acid residues of DYRK1A.

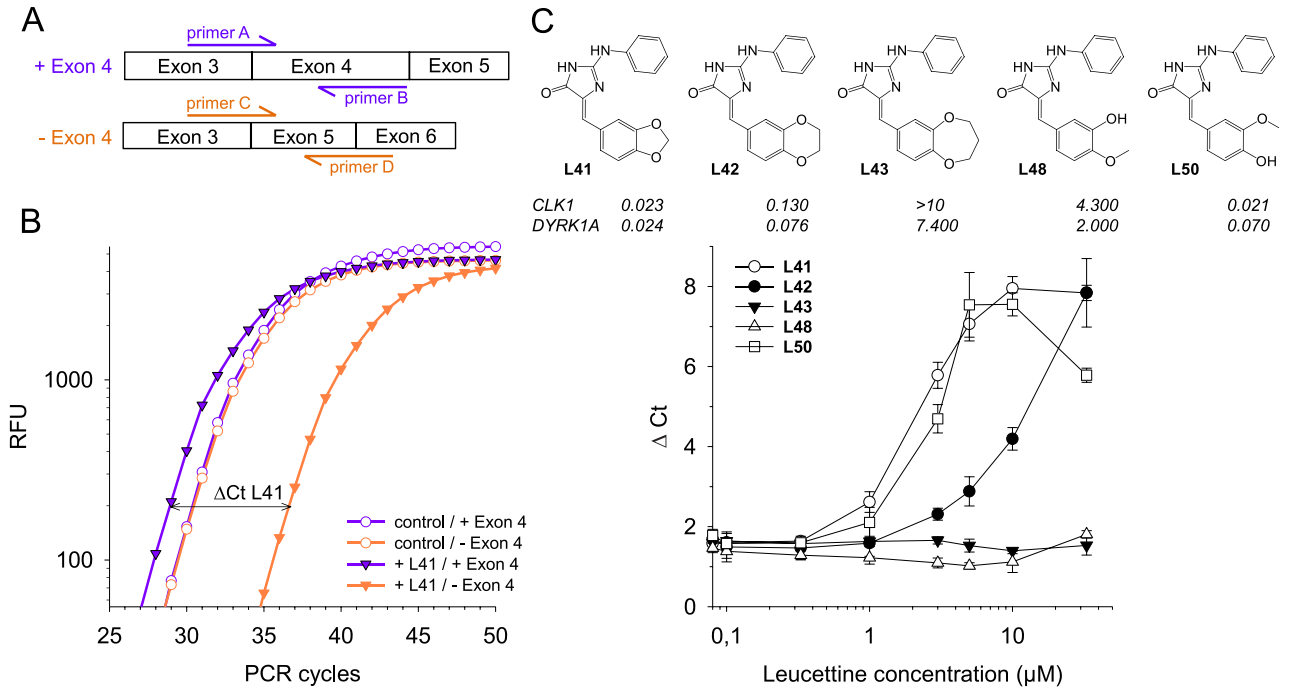

Figure 4. Leucettines modify CLK1 pre-mRNA splicing and trigger exon 4 inclusion. (A) qPCR products (+exon 4 and −exon 4) and their specific primers (primer pairs A/B and C/D, respectively) for the relative quantification of CLK1 splice variants (with or without exon 4, respectively). To avoid amplification due to genomic DNA contamination, primers A, C, and D span exon 3/exon 4, exon 3/exon 5, and exon 5/exon 6 junctions, respectively. Primer B anneals to exon 4. +Exon 4: 102 bp, −exon 4: 92 bp. (B) Quantification of CLK1 exon 4 inclusion from qPCR amplification data: example of ΔCt determination (Ct[−exon 4] − Ct[+exon 4]) for **L41**-treated HT22 cells (control: DMSO). Ct values were measured in the exponential phase at a fluorescence threshold of 200 RFU. (C) Dose−response curves for several representative Leucettines (**L41**, **L42**, **L43**, **L48**, **L50**). IC_{50} values (μM) toward CLK1 and DYRK1A are indicated under each structure. HT22 cells were treated at eight concentrations of each Leucettine (0, 0.1, 0.33, 1, 3, 5, 10, and 33 μM in 0.33% DMSO in triplicates) for 6 h, and CLK1 exon 4 inclusion was quantified by qPCR (ΔCt).

DYRK1A. Kinetics and dose−response studies (data not shown), performed with **L41**, showed a significant maximal inhibition (78%) of Tau Thr212 phosphorylation, which could not be further decreased by addition of pharmacological inhibitors of GSK-3 or CDKs (cyclin-dependent kinases) (data not shown). On the basis of these results, SH-SY5Y-Tau4R cells were exposed to each of the 68 Leucettines (10 μM, 6 h exposure) and analyzed for phospho-Thr212 levels relative to total Tau level (Tau5 antibody) (see the SI for methods). Results showed a clear-cut ability of Leucettines to inhibit Thr212 phosphorylation *in vitro* with, however, a modest correlation with in vitro DYRK1A inhibition (Tables 1−7). This limited correlation may be due to the phosphorylation of Thr212-Tau by other, unidentified kinases insensitive or poorly sensitive to Leucettines, to interactions of some Leucettines with alternative cellular (off-)targets, or to major differences in cell permeability among various Leucettines.

https://doi.org/10.1021/acs.jmedchem.1c01141
J. Med. Chem. 2022, 65, 1396−1417

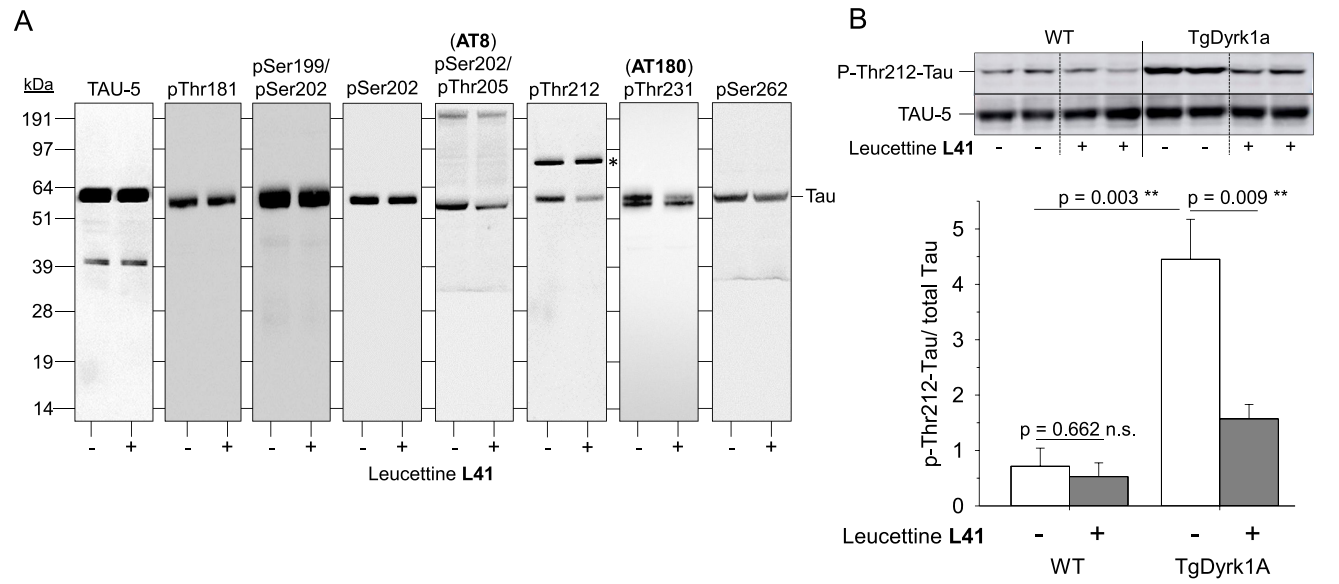

Figure 5. Leucettine L41 inhibits Tau phosphorylation at Thr212 in SH/SY5Y-Tau4R cells and in vivo. (A) SH/SY5Y-Tau4R cells were exposed to 10 μM **L41** or vehicle for 6 h. Proteins were extracted and resolved by SDS-PAGE followed by Western blotting with various antibodies: total Tau antibody (Tau-5) and antibodies specifically directed against Tau phosphorylated on Thr181, Ser199/Ser202, Ser202, Ser202/Thr205 (AT8), Thr212, Thr231 (AT180), or Ser262. pThr212-Tau specific antibodies cross-react specifically with Tau phosphorylated at Thr212 but also with a unique unspecific band (*) which can be used as a loading control. (B) pThr212-Tau levels in the brains of Tg(*Dyrk1a*) and wild-type (WT) mouse treated or not with **L41** (20 mg/kg, ip injection) (n = 4 per condition). pThr212-Tau is increased in brains of Tg(*Dyrk1a*) mice compared to controls (p = 0.003) and is significantly decreased when the transgenic mice are treated with **L41** (p = 0.009), but not in the wild-type animals (p = 0.662).

Tau phosphorylation is a key marker for DS and AD.[103,105−111] We therefore verified that Tau phosphorylation at one of its DYRK1A specific site, Thr212, was indeed inhibited by a Leucettine *in vivo*. As a first demonstration that DYRK1A is a major kinase phosphorylating this site in the brain, we showed that the mere expression of a single additional copy of the DYRK1A gene in Tg(*Dyrk1a*) mice resulted in an increase in brain Thr212-phosphorylated Tau compared to corresponding wild-type mice (Figure 5B). This result matches with the actual increase in DYRK1A mRNA, protein levels, and catalytic activity measured in brains of Tg(*Dyrk1a*) compared to brains of WT control animals.[25] When animals were treated with **L41** (20 mg/kg, daily ip injection for 19 days; pharmacokinetics studies showed that **L41** is not orally available (SI, Figure S5), thus requiring intraperitoneal (ip) administration), a reduction in phospho-Thr212-Tau was observed in the brains of Tg(*Dyrk1a*) animals (p = 0.009) compared to the brains of vehicle-treated animals but not in the brains of WT mice (p = 0.662, n.s.) (Figure 5B). This suggests that **L41** was able to cross the blood-brain barrier when administered ip, to reach and enter neuronal cells, and to inhibit endogenous DYRK1A (as also shown previously when the catalytic activity of endogenous brain DYRK1A was measured following immunoprecipitation[25]), resulting in reduced phosphorylation of its Tau substrate.

(4) Protection against Glutamate-Induced Cell Death. Excess release of extracellular glutamate in the central nervous system (excitotoxicity) contributes to the neurodegenerative processes observed in AD and stroke. Glutamate-induced cell death can be reconstituted in cell cultures and was shown to be prevented by **L41**[82] (Figure 6A). HT22 cells were exposed for 24 h to 10 mM glutamate in the absence or presence of a range of concentrations (up to 40 μM) of each of the 68 Leucettines. Some Leucettines prevented glutamate-induced cell death in a dose-dependent manner and their EC_{50} values (concentration providing 50% protection) were calculated. These values are reported in Tables 1−7. Dose−response curves for representative Leucettines, showing additivity of various substitutions, are shown in Figure 6B.

Results show that no correlation can be established between effective protection against glutamate-induced cell death and inhibition of any of the 11 kinases. Some unidentified kinase target(s) of the active Leucettines may be responsible for protection against glutamate-induced cell death. The possibility remains that some Leucettines were inactive on HT22 cells because of a lack of cell permeability or rapid intracellular metabolism. No conclusion can thus be drawn from such potentially kinase active, cell inactive molecules. In contrast, some kinase inactive molecules were clearly protecting HT22 cells from glutamate-induced cell death (**L51**, **L54** (Table 1), **L81**, **L82** (Table 7) (Figure 6B)), while some kinase active molecules were unable to provide protection from glutamate-induced cell death (e.g., **L64**, **L90**, **L91**, and **L92** (Table 7)).

Table 1 shows that protection against cell death tolerates quite a wide range of modifications of the benzodioxole ring system. EC_{50} values vary from 1.28 to 12.5 μM, with an open ring with a hydroxyl residue in the 7'a position (**L50**) providing the most efficacious activity (1.28 μM). The neuroprotection activity of Leucettines does not tolerate a substitution in 5'a (Table 2) or a modification of *N*1 (Table 3) or *N*3 (Tables 4, 5). In contrast, many modifications of the substituent *N*1" are tolerated or even improve this particular biological activity (Tables 6, 7) yet some annihilate the neuroprotective properties. No substitution (**L64**), single alkyl substitutions (**L31**, **L34**, **L66**), or dialkyl substitutions (**L68**-**L70**) of *N*1" lead to inactive compounds (Tables 6, 7). *N*1" substitution with a single phenyl leads to the active **L41**. The phenyl ring itself can (**L36**, **L39**, **L40**, **L74**, **L75**, **L80**−**L82**,

https://doi.org/10.1021/acs.jmedchem.1c01141
J. Med. Chem. 2022, 65, 1396−1417

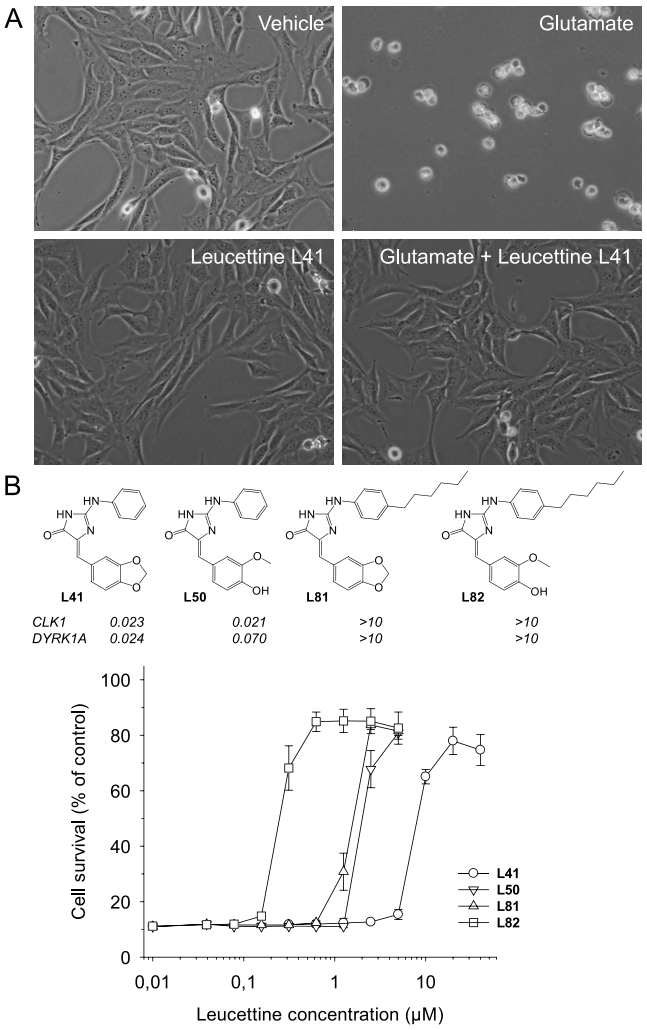

Figure 6. Leucettines prevent glutamate-induced cell death in mouse hippocampal HT22 cells. (A) Photographs (phase contrast microscope, CKX41, Olympus) of HT22 cells 24 h after exposure to vehicle, 10 μM **L41**, 10 mM glutamate, or both **L41** and glutamate. (B) Dose−response curves for several representative Leucettines (**L41**, **L50**, **L81**, **L82**). IC_{50} values (μM) toward CLK1 and DYRK1A are indicated under each structure. HT22 cells were exposed to various concentrations of each Leucettine and 10 mM glutamate. Their viability was assessed by the MTS assay 24 h after treatment and expressed as percentage of cell survival relative to control untreated cells.

L85−L87) or cannot (**L38**, **L83**, **L84**, **L90**) be substituted (Table 7). The most active compounds display a long alkyl chain in the *para*-position of the phenyl ring (**L80-L82**). Whether the phenyl is substituted or not, an open ring with a hydroxyl at 7'a is more active than the corresponding benzodioxole ring (compare **L50** with **L41**, and **L82** with **L81**) (Figure 6B). The *N*1" phenyl itself can be substituted with a second ring system. Biphenyl (**L83**) and bipiperidine (**L84**) substitutions on *N*1" lead to inactive compounds. In contrast, phenyl-piperidine (**L85**, **L86**) substitutions lead to biologically active molecules. Phenyl-piperazine substitutions are also active (**L87**, **L88**) as long as the *para*-nitrogen is not substituted (**L90−L92**). The most active compounds with a double ring system are **L85** and **L87**.

HT22 cells were exposed to each of the 68 Leucettines at 20 μM for 24 h. Cell survival, assessed using the classic MTS (3-(4,5-dimethylthiazol-2-yl)-5-(3-carboxymethoxyphenyl)-2-(4-sulfophenyl)-2*H*-tetrazolium) assay, showed a lack of deleterious effects of the whole family of Leucettines at this concentration (Tables 1−7).

(5) Induction of Autophagy. We reported that Leucettines induce activation of phosphatidylinositol-3-kinase (PI3K)/mTor-dependent autophagy.[83] U-2 OS cells were exposed to 10 μM of each of the 68 Leucettines for 4 h, and autophagy was assessed by counting the number of LC3 (microtubule associated protein light chain 3) foci per cell, a hallmark of autophagy. DMSO and rapamycin were used as negative and positive controls, respectively. Antibodies against lysosomal-associated membrane protein 1 (LAMP-1) were used to detect lysosomes and DAPI to stain DNA. Figure 7 illustrates representative results obtained with **L41** and **L50**. SAR results (Tables 1−7) showed that most Leucettines (such as **L36**, **L37**, **L41**, **L44**, **L50**, **L76**, **L90−L92**) inducing autophagy inhibited CLKs with high efficiency. However, a few autophagy inducing compounds (**L46**, **L53**, **L85**, **L86**, **L93**) displayed modest or no kinase inhibitory activity, suggesting mechanisms other than kinase inhibition. Leucettines that were inactive or poorly active on kinases were mostly unable to trigger autophagy. A good example is shown with the isomeric Leucettines **L48** and **L50**, which, respectively, display low or high kinase inhibition and low or high autophagy induction properties. However, some potent kinase inhibitory Leucettines (such as **L31**, **L34**, **L39**, **L40**, **L59**, **L63**, **L64**, **L73**, **L74**, **L75**) were unable to trigger autophagy, suggesting independent, alternative mechanisms of action or poor cell permeability.

Little correlation was observed between the ability to alter CLK1 pre-mRNA splicing and induction of autophagy: for example, compounds **L46**, **L36**, **L85**, **L86**, and **L92** are potent autophagy inducers and only modestly modify exon 4 inclusion. Inversely, compounds **L21**, **L31**, **L39**, **L40**, **L74**, **L75**, and **L78** alter CLK1 splicing but do not induce autophagy. No correlation was seen between the abilities to alter CLK1 pre-mRNA splicing and to protect against glutamate-induced cell death: for example, compounds **L80−L82** and **L85−L88**, which are the most potent protectors, do not alter splicing. siRNA-mediated inactivation of CLK1, but not of DYRK1A, promoted autophagy, suggesting that CLK inhibition, but not DYRK inhibition, might contribute to autophagy induction,[83] a trend confirmed with pharmacological inhibitors of these kinases.[83,112,113]

(6) Antagonism of the CB1 Cannabinoid Receptor. To investigate the selectivity of Leucettines and to identify potential secondary targets, we submitted **L41** (10 μM) to the DiscoveRx PathHunter β-arrestin enzyme fragment complementation based GPCR screen. **L41** was tested both for agonist or antagonist activity on 158 known GPCRs and for potential agonist activity on 76 orphan GPCRs (Figure 8A). Results showed that **L41** displayed not a single agonist activity on either known or orphan GPCRs. In contrast, **L41** strongly antagonized CP-55940-induced CB1 activity (98% inhibition). With the exception of Adenosine A_3 receptor (ADORA3) (45% inhibition with 10 μM **L41**), no other GPCR activity was found to be antagonized by **L41**. We next tested all 68 Leucettines at 10 μM for their potential ability to antagonize CB1 activated by CP-55940 (Tables 1−7). Most Leucettines were found to be inactive. We then ran dose−response curves for 11 Leucettines, **L0**, **L37**, **L41**, **L43**, **L50**, **L54**, **L68**, **L82**, **L85**, **L86**, and **L92** (Tables 1−7). Leucettines fall in four categories (Tables 1−7): (i) active on both kinases and CB1

https://doi.org/10.1021/acs.jmedchem.1c01141
J. Med. Chem. 2022, 65, 1396−1417

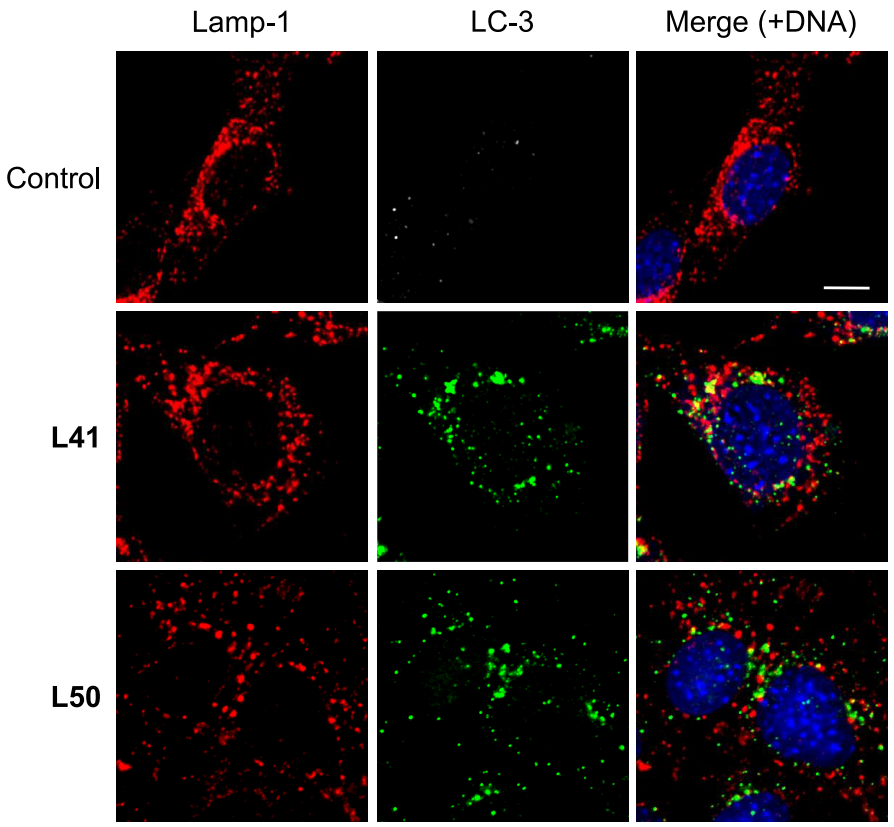

Figure 7. Leucettines trigger LC-3 modification and autophagy in mouse hippocampal HT22 cells. Immunofluorescence images of HT22 cells treated for 24 h with 10 μM of the indicated Leucettine (**L41**, **L50**) or DMSO vehicle (control). Cells were stained for Lamp-1 (red) and LC-3 (green) with specific antibodies. DNA (blue) was visualized using DAPI. Bar is 10 μm.

(**L41**, **L42**, **L36**, **L39**, **L40**, **L44**), (ii) inactive on both kinases and CB1 (**L32**, **L56**, **L60**), (iii) inactive on kinases and active on CB1 (**L43**, **L53**, **L54**, **L81**, **L82**, **L85**), and (iv) active on kinases and inactive on CB1 (**L0**, **L37**, **L50**, **L59**, **L64**, **L76**, **L90-L92**). Results clearly showed that the CB1 antagonism activity depends on structural features that are independent from the structural requirements for kinase inhibition. Key modifications for potent CB1 antagonism included no substitution on 5′a (compare **L56** and **L41**, Table 2), a nitrogen and not a sulfur at position *N*1 (compare **L58** and **L41**, Table 3), unsubstituted *N*3 (compare **L21** and **L41**, Table 5), one but not two substitutions on *N*1" (compare **L67** and **L41**, Table 6), some specific substitutions on *N*1" phenyl (−F (**L74**, **L75**), −O−CH_3 (**L38**), −CH_3 (**L36**), some (**L77**, **L78**) but not all (**L79**) di-CH_3, -piperidine (**L85**, **L86**), but not −OH (**L37**, **L76**, Table 7). In contrast, substitution of the *N*1" phenyl with a piperazine (**L87**−**L89**) or a *N*-methyl-piperazine (**L90**−**L92**) completely abolished the CB1 antagonism activity. Altogether these results showed that it is possible to develop Leucettines with strong kinase inhibitory activity but no CB1 antagonism, the most desired feature. Previous results showed that a CB1 antagonist inactive on DYRK1A (**L92** (unfortunately labeled **L99** in ref 25) was unable to correct cognitive deficits in a DS mouse model, in contrast to a DYRK1A inhibitor inactive on CB1 (**L41**).[25]

We next investigated the allosteric effect of selected Leucettines on the cannabinoid receptor 1. The allosteric parameters (K_B and α) of four compounds, **L41**, **L43**, **L85** and **L92**, were evaluated in the presence of the orthosteric agonist CP-55940, and the data, in comparison with DYRK1A inhibition and CB1 arrestin results, are summarized in Figure 8B. Three compounds **L41**, **L43**, and **L85** showed an allosteric impact on orthosteric agonist CP-55940 binding with K_B values of 2.2, 1.2, and 3.3 μM, respectively. However, no allosteric effect on CP-55940 binding was observed for **L92**, in agreement with the CB1 arrestin assay. **L41**, **L85**, and **L92** were potent DYRK1A inhibitors, while **L43** was marginally inhibitory, again highlighting the fact that DYRK1A inhibition and CB1 antagonism are not necessarily linked in the Leucettine family.

Three compounds, **L41**, **L43**, and **L85**, that showed positive allosteric modulation on orthosteric agonist binding of the CB1 receptor were further tested for their impact on G-protein coupling induced by CP-55940 (Figure 8C). Unlike many positive allosteric modulators,[114] but comparable to the CB1 allosteric modulator ORG27569,[115,116] these compounds showed a substantial, concentration-dependent inhibition of CP-55940-induced GTPγS binding, as compared to control (vehicle only).

CONCLUSION

Over 40 DYRKs/CLKs inhibitors (most DYRKs inhibitors inhibit CLKs) have been described in the literature (reviews in refs 14, 16, 20, 33, 69). These medicinal chemistry efforts have been encouraged by the involvement of both families of kinases in multiple human diseases as briefly described in the introduction (review in ref 16). Our focus on DYRK1A as a therapeutic target is motivated by the potential clinical benefits of DYRK1A inhibitors in the treatment of cognitive deficits, memory, and learning, associated with DS and AD, but also in

https://doi.org/10.1021/acs.jmedchem.1c01141
J. Med. Chem. 2022, 65, 1396−1417

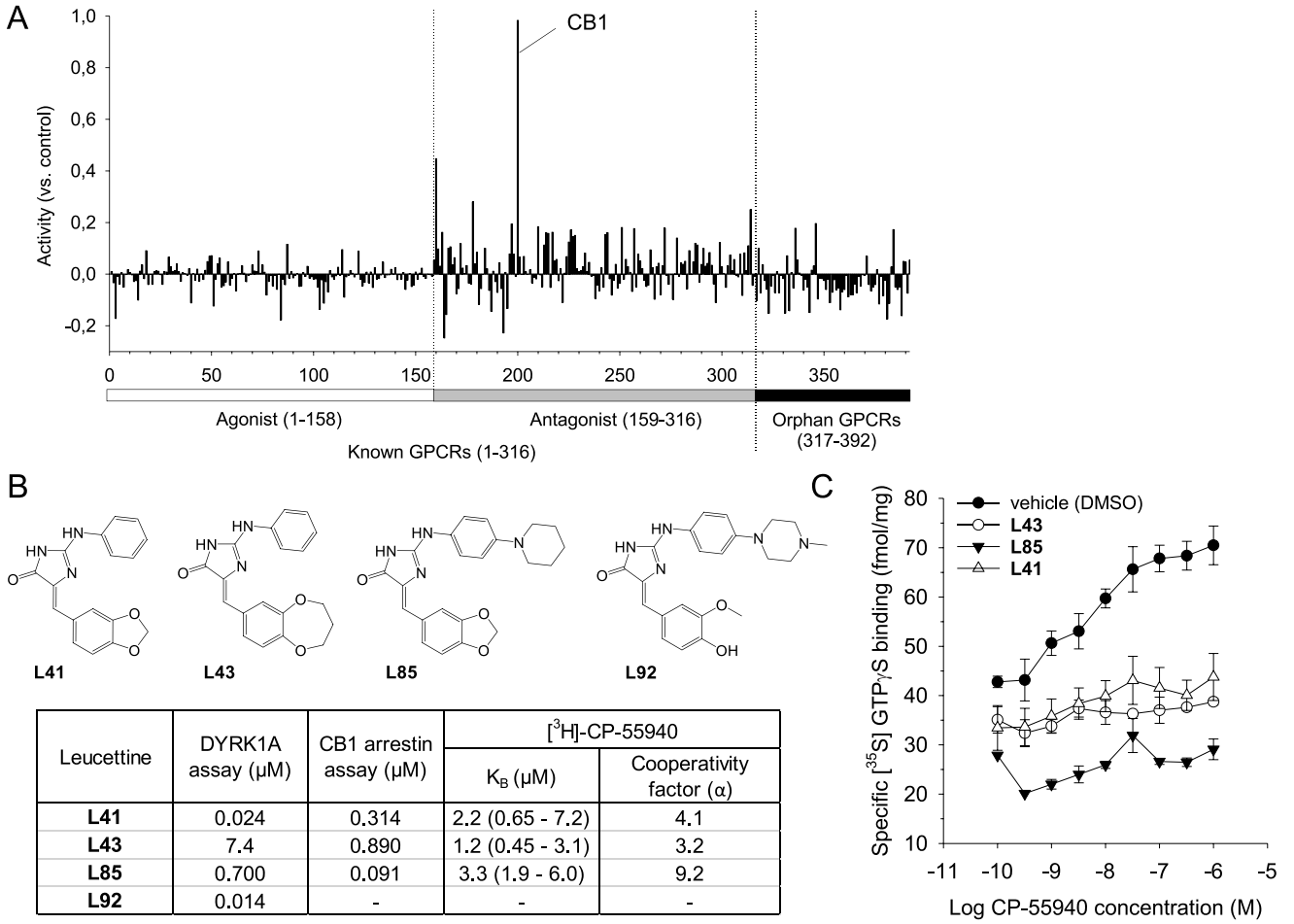

Leucettine	DYRK1A assay (μM)	CB1 arrestin assay (μM)	[3H]-CP-55940	
			K_B (μM)	Cooperativity factor (α)
L41	0.024	0.314	2.2 (0.65 - 7.2)	4.1
L43	7.4	0.890	1.2 (0.45 - 3.1)	3.2
L85	0.700	0.091	3.3 (1.9 - 6.0)	9.2
L92	0.014	-	-	-

Figure 8. Some Leucettines interact with the cannabinoid receptor CB1. (A) **L41** was tested at 10 μM as a potential agonist or antagonist of 158 known GPCRs and as a potential agonist for 76 orphan GPCRs, using the DiscoveRx PathHunter β-arrestin enzyme fragment complementation technology. Activity is represented as percent of control GPCR activity in the absence (potential agonist activity) or presence (potential antagonist activity) of appropriate GPCR agonists. CB1, cannabinoid receptor 1. (B) Structure and effects of four Leucettines (**L41**, **L43**, **L85**, **L92**) on DYRK1A activity (IC_{50} values in μM) and CB1 receptor arrestin activity in the presence of a CB1 agonist, CP-55940 (IC_{50} values in μM) (DiscoveRx) and binding parameters to CB1 receptor. Data are the median and corresponding 95% confidence limits from at least three independent experiments performed in duplicate. K_B and cooperativity factor for the compounds were determined using [^{3}H]-CP-55940. −, no DYRK1A nor CB1 arrestin inhibition, or no significant change in [^{3}H]-CP-55940 binding observed up to 10 μM. (C) Effect of **L41**, **L43**, **L85**, and vehicle on CP-55940-induced GTPγS binding to cell membranes expressing the CB1 receptor. Dose−response curves for CP-55940 induced [^{35}S]-GTPγS binding in cell membrane preparations expressing the CB1 receptor in the absence or presence of 10 μM of each Leucettine. Nonspecific binding was determined in the presence of 10 μM unlabeled GTPγS. Each data point represents the mean ± SE (error bars) of at least three independent experiments performed in duplicate.

their potential to address reduced β-cell mass and insufficient insulin production seen in type I and type II diabetes. Following the screening of a high diversity library of over 50 000 low molecular weight molecules on recombinant DYRK1A, we identified the marine natural product Leucettamine B as an initial hit of potential interest.[76−81] We next synthesized a library of >500 Leucettamine B analogues, collectively named Leucettines,[81−84] from which Leucettine **L41** was selected as a lead compound. Proof-of-concept studies were carried out with **L41**, showing that pharmacological inhibition of DYRK1A was able to correct learning and memory deficits in three animal models of DS[25] and three animal models of AD (refs 39, 72; Meijer et al., unpublished). We selected a series of 68 Leucettines in our library to describe their SAR in a variety of biological assays.

In terms of *in vitro* kinase inhibition, the SAR correlates very well with the crystal structure of **L41** in complex with DYRK1A, DYRK2, and CLK3.[81,82] The SAR also correlates with the sequence conservation among DYRKs and CLKs (SI Tables S1, S2 and Figure S4). The most potent inhibitors (**L90**, **L91**, **L92**) reached 7−14 nM IC_{50} values. DYRK1A, DYRK1B, DYRK2, CLK1, CLK2, and CLK4 were closely related in terms of sensitivity to Leucettines. Further optimization is under way based on alterations of both sides (aminoimidazolone and benzodioxole) of the Leucettine scaffold. The relationship between kinase inhibition and cellular effects shows that, within a relatively homogeneous chemical family such as Leucettines, diverse SARs coexist depending on the biological effects evaluated. It is quite difficult to correlate a specific biological effect to the inhibition of a single kinase. In fact, biological effects probably originate from the combined effect of individual Leucettines on a subset of DYRKs and CLKs. We should be humble when attributing a specific biological effect of a product to a specific target!

When the effects of Leucettines were tested on CLK1 splicing in cultured cells, a good correlation was seen, with a

https://doi.org/10.1021/acs.jmedchem.1c01141
J. Med. Chem. 2022, 65, 1396−1417

few exceptions, between DYRKs and CLKs inhibition potency and alternative splicing of CLK1 mRNA. Tau phosphorylation at Thr212 is known to be catalyzed by DYRK1A,[102,103] yet there was a relatively modest correlation between the potency of Leucettines at inhibiting this kinase *in vitro* and the reduction of phospho-Thr212-Tau levels in cells. Nevertheless, **L41** treatment of a DS mouse model led to the reduction of brain Tau phosphorylation at the Thr212 site.

Three other biological activities sensitive to some Leucettines showed a very different SAR pattern, with some kinase-inactive Leucettines being very potent in these assays and some kinase-active Leucettines showing low or no activity in these biological assays. Glutamate-induced cell death was initially found to be prevented by a cotreatment with Leucettine **L41** (Figure 6A). However, the SAR study rapidly showed a lack of correlation between kinase inhibition (at least among the 11 kinases tested in this study) and protection against glutamate-induced cell death. It would be of interest to screen the most active Leucettines in this assay on a wide panel of kinases to find out whether they inhibit some other kinases which might be involved in glutamate-induced cell death. We feel it would be interesting to engage a medicinal chemistry effort, driven by this simple biological assay, to develop more potent Leucettines protecting against glutamate-induced excitotocity, an area of wide interest in various CNS diseases such as AD, Huntington's disease, lateral amyotrophic sclerosis, PD, stroke, and traumatic brain injury. The cellular assays of autophagy induction by Leucettines showed very modest correlation, with numerous counter-examples, with inhibition of DYRKs or CLKs. Again, it would be interesting to investigate the kinase selectivity of the best autophagy-inducing Leucettines to see if they inhibit some other kinases involved in this cellular process. It would also be of interest to optimize a subfamily of Leucettines on the basis of autophagy induction, an area of potential applications in neurodegenerative diseases. The finding of the Leucettines' effects on ligand-activated cannabinoid receptor CB1 stemmed from a screen on a wide panel of GPCRs (Figure 8A). Kinase inhibition and CB1 receptor antagonism do not appear to be correlated. It may thus be possible to develop Leucettine subfamilies that are exclusively specific for DYRK1A or for CB1 or that combine both activities. This might be of potential interest in view of the recently described beneficial effects of CB1 antagonism in two DS models.[117] **L41** carries both DYRK1A inhibition and CB1 antagonism and corrects spatial memory deficits in three mouse models of DS.[25] **L43**, which does not inhibit DYRK1A and has modest activity on CB1, does not restore cognitive functions.[25] In contrast, **L92** (mistakenly named **L99** in ref 25), which is a potent DYRK1A inhibitor but has no antagonistic effects on CB1, restores cognitive functions, demonstrating that DYRK1A inhibition is key in the cognition correcting effects of Leucettines.[25]

In conclusion, the Leucettine scaffold provides several opportunities to develop drug candidates with different biological targets and activities and thus potential applications in different pathologies.

EXPERIMENTAL PROCEDURES

All chemistry and biological experimental procedures are provided in detail in the Supporting Information. The purity of the synthesized Leucettines was determined by high resolution mass spectroscopy and microanalysis. The purity was >95% in all cases.

ASSOCIATED CONTENT

Supporting Information

The Supporting Information is available free of charge at https://pubs.acs.org/doi/10.1021/acs.jmedchem.1c01141.

Chemistry section describing general methods, synthesis protocols, and molecular formula strings for each Leucettine; biology section divided in three subsections: (1) biochemistry (protein kinase assays; allosteric modulation of CB1), (2) cell biology (HT22 cell culture and survival assessment; CLK1 alternative splicing in HT22 cells; Tau phosphorylation in SH-SY5Y-Tau4R cells; autophagy assessment in HT22 cells; GPCR selectivity panel), and (3) in vivo studies in mice (animals handling and treatment; in vivo Thr212-Tau phosphorylation level assessment) (PDF)

Molecular formula strings (CSV)

AUTHOR INFORMATION

Corresponding Author

Laurent Meijer − *Manros Therapeutics & Perha Pharmaceuticals, Perharidy Research Center, 29680 Roscoff, Bretagne, France;* orcid.org/0000-0003-3511-4916; Email: meijer@perha-pharma.com

Authors

Tania Tahtouh − *Manros Therapeutics & Perha Pharmaceuticals, Perharidy Research Center, 29680 Roscoff, Bretagne, France; CNRS, 'Protein Phosphorylation and Human Disease' Group, Station Biologique De Roscoff, 29682 Roscoff, Bretagne, France; College Of Health Sciences, Abu Dhabi University, Abu Dhabi, United Arab Emirates*

Emilie Durieu − *Manros Therapeutics & Perha Pharmaceuticals, Perharidy Research Center, 29680 Roscoff, Bretagne, France; CNRS, 'Protein Phosphorylation and Human Disease' Group, Station Biologique De Roscoff, 29682 Roscoff, Bretagne, France*

Benoît Villiers − *Manros Therapeutics & Perha Pharmaceuticals, Perharidy Research Center, 29680 Roscoff, Bretagne, France*

Céline Bruyère − *Manros Therapeutics & Perha Pharmaceuticals, Perharidy Research Center, 29680 Roscoff, Bretagne, France*

Thu Lan Nguyen − *Manros Therapeutics & Perha Pharmaceuticals, Perharidy Research Center, 29680 Roscoff, Bretagne, France; Institut De Génétique Et De Biologie Moléculaire et Cellulaire, Department of Translational Medicine and Neurogenetics, Université de Strasbourg, CNRS UMR7104 & INSERM U964, 67400 Illkirch, France; Laboratory of Molecular & Cellular Neuroscience, The Rockefeller University, New York, New York 10021-6399, United States*

Xavier Fant − *CNRS, 'Protein Phosphorylation and Human Disease' Group, Station Biologique De Roscoff, 29682 Roscoff, Bretagne, France*

Kwang H. Ahn − *Department of Pharmaceutical Sciences, University of Connecticut, Storrs, Connecticut 06269, United States*

Leepakshi Khurana − *Department of Pharmaceutical Sciences, University of Connecticut, Storrs, Connecticut 06269, United States*

https://doi.org/10.1021/acs.jmedchem.1c01141
J. Med. Chem. 2022, 65, 1396−1417

Emmanuel Deau − *Manros Therapeutics & Perha Pharmaceuticals, Perharidy Research Center, 29680 Roscoff, Bretagne, France*
Mattias F. Lindberg − *Manros Therapeutics & Perha Pharmaceuticals, Perharidy Research Center, 29680 Roscoff, Bretagne, France*
Elodie Sévère − *Manros Therapeutics & Perha Pharmaceuticals, Perharidy Research Center, 29680 Roscoff, Bretagne, France*
Frédéric Miege − *Edelris, 69008 Lyon, France*
Didier Roche − *Edelris, 69008 Lyon, France*
Emmanuelle Limanton − *Institut des Sciences Chimiques de Rennes ISCR-UMR CNRS 6226, Université de Rennes 1, Campus de Beaulieu, 35042 Rennes Cedex, France*
Jean-Martial L'Helgoual'ch − *Institut des Sciences Chimiques de Rennes ISCR-UMR CNRS 6226, Université de Rennes 1, Campus de Beaulieu, 35042 Rennes Cedex, France*
Guillaume Burgy − *Manros Therapeutics & Perha Pharmaceuticals, Perharidy Research Center, 29680 Roscoff, Bretagne, France; Institut des Sciences Chimiques de Rennes ISCR-UMR CNRS 6226, Université de Rennes 1, Campus de Beaulieu, 35042 Rennes Cedex, France*
Solène Guiheneuf − *Institut des Sciences Chimiques de Rennes ISCR-UMR CNRS 6226, Université de Rennes 1, Campus de Beaulieu, 35042 Rennes Cedex, France*
Yann Herault − *Institut De Génétique Et De Biologie Moléculaire et Cellulaire, Department of Translational Medicine and Neurogenetics, Université de Strasbourg, CNRS UMR7104 & INSERM U964, 67400 Illkirch, France*
Debra A. Kendall − *Department of Pharmaceutical Sciences, University of Connecticut, Storrs, Connecticut 06269, United States*
François Carreaux − *Institut des Sciences Chimiques de Rennes ISCR-UMR CNRS 6226, Université de Rennes 1, Campus de Beaulieu, 35042 Rennes Cedex, France;* orcid.org/0000-0002-7406-8353
Jean-Pierre Bazureau − *Institut des Sciences Chimiques de Rennes ISCR-UMR CNRS 6226, Université de Rennes 1, Campus de Beaulieu, 35042 Rennes Cedex, France*

Complete contact information is available at: https://pubs.acs.org/10.1021/acs.jmedchem.1c01141

Author Contributions

[†]T.T. and E.D.: Equal contributions of the two first authors.

Notes

The authors declare the following competing financial interest(s): L. Meijer, J.P. Bazureau and F. Carreaux are co-inventors on the Leucettines patent. L. Meijer is president and CSO of Perha Pharmaceuticals which develops Leucettines and related DYRK1A inhibitors. The other authors declare no competing financial interest.

■ ACKNOWLEDGMENTS

This article is dedicated to the memory of Bernard Jégou. Preclathridine A and clathridine A were kindly provided by Dr. Carl Lovely (University of Texas at Arlington, USA). Recombinant CK1 was generously provided by Dr. Claude Cochet (INSERM U1036, Grenoble, France). HT22 cells and SH-SY5Y-Tau4R cells were gifts from Dr. David Schubert (Salk Institute, La Jolla, CA) and Dr. Fred Van Leuven (Leuven, Belgium), respectively. This research was supported by grants from the "Fondation Jérôme Lejeune" (LM), the "Agence Nationale pour la Recherche (ANR)" (DYRK-DOWN) (LM, YH), the "Fonds Unique Interministériel" (FUI) PHARMASEA and TRIAD (LM, JPB, FC) projects, an FP7-KBBE-2012 grant (BlueGenics). This project has received funding from the European Union's Horizon 2020 research and innovation programme under grant agreement No 848077 (GO-DS21). This reflects only the authors' view and the European Commission is not responsible for any use that may be made of the information it contains.

■ ABBREVIATIONS

AD, Alzheimer's disease;; ALL, acute lymphoblastic leukemia; AMKL, acute megakaryoblastic leukemia; CDKs, cyclin-dependent kinases; CK2, casein kinase 2; CLKs, cdc2-like kinases; CB1, cannabinoid receptor 1; DMSO, dimethyl sulfoxide; DS, Down syndrome; DSCR, Down syndrome critical region; DYRKs, dual specificity, tyrosine phosphorylation regulated kinases; gHSQMBC, gradient heteronuclear single quantum multiple bond correlation; GPCRs, G-protein coupled receptors; GSK-3, glycogen synthase kinase-3; ip, intraperitoneal; LAMP-1, lysosomal-associated membrane protein 1; LC3, microtubule associated protein light chain 3; MRD7, Mental retardation disease 7; MTS, 3-(4,5-dimethylthiazol-2-yl)-5-(3-carboxymethoxyphenyl)-2-(4-sulfophenyl)-2*H*-tetrazolium; PD, Parkinson's disease; PI3K, phosphatidylinositol-3-kinase; SAR, structure−activity relationship; SRp, serine/arginine-rich proteins; TBAF, tetrabutylammonium fluoride; TBHP, *tert*-butyl hydroperoxide.

■ REFERENCES

(1) Manning, G.; Whyte, D. B.; Martinez, R.; Hunter, T.; Sudarsanam, S. The protein kinase complement of the human genome. *Science* **2002**, *298*, 1912−1934.
(2) Roskoski, R. 2015. A historical overview of protein kinases and their targeted small molecule inhibitors. *Pharmacol. Res.* **2015**, *100*, 1.
(3) Wilson, L. J.; Linley, A.; Hammond, D. E.; Hood, F. E.; Coulson, J. M.; MacEwan, D. J.; Ross, S. J.; Slupsky, J. R.; Smith, P. D.; Eyers, P. A.; Prior, A. New perspectives, opportunities, and challenges in exploring the human protein kinome. *Cancer Res.* **2018**, *78*, 15−29.
(4) Zhang, H.; Cao, X.; Tang, M.; Zhong, G.; Si, Y.; Li, H.; Zhu, F.; Liao, Q.; Li, L.; Zhao, J.; Feng, J.; Li, S.; Wang, C.; Kaulich, M.; Wang, F.; Chen, L.; Li, L.; Xia, Z.; Liang, T.; Lu, H.; Feng, X. H.; Zhao, B. A subcellular map of the human kinome. *eLife* **2021**, *10*, No. e64943.
(5) Wu, P.; Nielsen, T. E.; Clausen, M. H. FDA-approved small-molecule kinase inhibitors. *Trends Pharmacol. Sci.* **2015**, *36*, 422−439.
(6) Müller, S.; Chaikuad, A.; Gray, N. S.; Knapp, S. The ins and outs of selective kinase inhibitor development. *Nat. Chem. Biol.* **2015**, *11*, 818−821.
(7) Elkins, J. M.; Fedele, V.; Szklarz, M.; Abdul Azeez, K. R.; Salah, E.; Mikolajczyk, J.; Romanov, S.; Sepetov, N.; Huang, X. P.; Roth, B. L.; Al Haj Zen, A.; Fourches, D.; Muratov, E.; Tropsha, A.; Morris, J.; Teicher, B. A.; Kunkel, M.; Polley, E.; Lackey, K. E.; Atkinson, F. L.; Overington, J. P.; Bamborough, P.; Müller, S.; Price, D. J.; Willson, T. M.; Drewry, D. H.; Knapp, S.; Zuercher, W. J. Comprehensive characterization of the published kinase inhibitor set. *Nat. Biotechnol.* **2016**, *34*, 95−103.
(8) Roskoski, R. Properties of FDA-approved small molecule protein kinase inhibitors. *Pharmacol. Res.* **2019**, *144*, 19−50.
(9) Roskoski, R. Properties of FDA-approved small molecule protein kinase inhibitors: A 2020 update. *Pharmacol. Res.* **2020**, *152*, 104609.
(10) Roskoski, R. Properties of FDA-approved small molecule protein kinase inhibitors: A 2021 Update. *Pharmacol. Res.* **2021**, *165*, 105463.
(11) Aranda, S.; Laguna, A.; de la Luna, S. DYRK family of protein kinases: evolutionary relationships, biochemical properties, and functional roles. *FASEB J.* **2011**, *25*, 449−462.

(12) Abbassi, R.; Johns, T. G.; Kassiou, M.; Munoz, L. DYRK1A in neurodegeneration and cancer: Molecular basis and clinical implications. *Pharmacol. Ther.* **2015**, *151*, 87−98.
(13) Kay, L. J.; Smulders-Srinivasan, T. K.; Soundararajan, M. Understanding the multifaceted role of human Down syndrome kinase DYRK1A. *Adv. Protein Chem. Struct. Biol.* **2016**, *105*, 127−171.
(14) Pathak, A.; Rohilla, A.; Gupta, T.; Akhtar, M. J.; Haider, M. R.; Sharma, K.; Haider, K.; Yar, M. S. DYRK1A kinase inhibition with emphasis on neurodegeneration: a comprehensive evolution story-cum-perspective. *Eur. J. Med. Chem.* **2018**, *158*, 559−592.
(15) Arbones, M. L.; Thomazeau, A.; Nakano-Kobayashi, A.; Hagiwara, M.; Delabar, J. M. DYRK1A and cognition: a lifelong relationship. *Pharmacol. Ther.* **2019**, *194*, 199−221.
(16) Lindberg, M.; Meijer, L. Dual-specificity, tyrosine phosphorylation-regulated kinases (DYRKs) and cdc2-like kinases (CLKs) in human disease, an overview. *Int. J. Mol. Sci.* **2021**, *22*, 6047.
(17) Nayler, O.; Stamm, S.; Ullrich, A. Characterization and comparison of four serine- and arginine-rich (SR) protein kinases. *Biochem. J.* **1997**, *326*, 693−700.
(18) Singh, R. K.; Cooper, T. A. Pre-mRNA splicing in disease and therapeutics. *Trends Mol. Med.* **2012**, *18*, 472−482.
(19) Jain, P.; Karthikeyan, C.; Moorthy, N. S.; Waiker, D. K.; Jain, A. K.; Trivedi, P. Human CDC2-like kinase 1 (CLK1): a novel target for Alzheimer's disease. *Curr. Drug Targets* **2014**, *15*, 539−550.
(20) Martín Moyano, P.; Němec, V.; Paruch, K. Cdc-like kinases (CLKs): biology, chemical probes, and therapeutic potential. *Int. J. Mol. Sci.* **2020**, *21*, 7549.
(21) Becker, W.; Soppa, U.; Tejedor, F. J. DYRK1A: a potential drug target for multiple Down syndrome neuropathologies. *CNS Neurol. Disord.: Drug Targets* **2014**, *13*, 26−33.
(22) Duchon, A.; Herault, Y. DYRK1A, a dosage-sensitive gene involved in neurodevelopmental disorders, is a target for drug development in Down syndrome. *Front. Behav. Neurosci.* **2016**, *10*, 104.
(23) Stringer, M.; Goodlett, C. R.; Roper, R. J. Targeting trisomic treatments: optimizing Dyrk1a inhibition to improve Down syndrome deficits. *Mol. Genet. Genomic Med.* **2017**, *5*, 451−465.
(24) Feki, A.; Hibaoui, Y. DYRK1A protein, a promising therapeutic target to improve cognitive deficits in Down syndrome. *Brain Sci.* **2018**, *8*, 187.
(25) Nguyen, T. L.; Duchon, A.; Manousopoulou, A.; Loaëc, N.; Villiers, B.; Pani, G.; Karatas, M.; Mechling, A. E.; Harsan, L. A.; Limanton, E.; Bazureau, J. P.; Carreaux, F.; Garbis, S. D.; Meijer, L.; Hérault, Y. Correction of cognitive deficits in mouse models of Down syndrome by pharmacological inhibitor of DYRK1A. *Dis. Models & Mech.* **2018**, *11*, dmm035634.
(26) Kurabayashi, N.; Nguyen, M. D.; Sanada, K. Triple play of DYRK1A kinase in cortical progenitor cells of Trisomy 21. *Neurosci. Res.* **2019**, *138*, 19−25.
(27) Rueda, N.; Flórez, J.; Dierssen, M.; Martínez-Cué, C. Translational validity and implications of pharmacotherapies in preclinical models of Down syndrome. *Prog. Brain Res.* **2020**, *251*, 245−268.
(28) Evers, J. M. G.; Laskowski, R. A.; Bertolli, M.; Clayton-Smith, J.; Deshpande, C.; Eason, J.; Elmslie, F.; Flinter, F.; Gardiner, C.; Hurst, J. A.; Kingston, H.; Kini, U.; Lampe, A. K.; Lim, D.; Male, A.; Naik, S.; Parker, M. J.; Price, S.; Robert, L.; Sarkar, A.; Straub, V.; Woods, G.; Thornton, J. M.; Wright, C. F. Structural analysis of pathogenic mutations in the DYRK1A gene in patients with developmental disorders. *Hum. Mol. Genet.* **2017**, *26*, 519−526.
(29) Widowati, E. W.; Ernst, S.; Hausmann, R.; Müller-Newen, G.; Becker, W. Functional Characterization of DYRK1A missense variants associated with *a* syndromic form of intellectual deficiency and autism. *Biol. Open* **2018**, *7*, bio032862.
(30) Ferrer, I.; Barrachina, M.; Puig, B.; Martínez de Lagrán, M.; Martí, E.; Avila, J.; Dierssen, M. Constitutive Dyrk1A is abnormally expressed in Alzheimer disease, Down syndrome, Pick disease, and related transgenic models. *Neurobiol. Dis.* **2005**, *20*, 392−400.
(31) Kimura, R.; Kamino, K.; Yamamoto, M.; Nuripa, A.; Kida, T.; Kazui, H.; Hashimoto, R.; Tanaka, T.; Kudo, T.; Yamagata, H.; Tabara, Y.; Miki, T.; Akatsu, H.; Kosaka, K.; Funakoshi, E.; Nishitomi, K.; Sakaguchi, G.; Kato, A.; Hattori, H.; Uema, T.; Takeda, M. The DYRK1A gene, encoded in chromosome 21 Down Syndrome Critical Region, bridges between *β*-Amyloid production and Tau phosphorylation in Alzheimer disease. *Hum. Mol. Genet.* **2007**, *16*, 15−23.
(32) Jin, N.; Yin, X.; Gu, J.; Zhang, X.; Shi, J.; Qian, W.; Ji, Y.; Cao, M.; Gu, X.; Ding, F.; Iqbal, K.; Gong, C. X.; Liu, F. Truncation and activation of Dual Specificity Tyrosine Phosphorylation-Regulated Kinase 1A by calpain I: A molecular mechanism linked to tau pathology in alzheimer disease. *J. Biol. Chem.* **2015**, *290*, 15219−15237.
(33) Stotani, S.; Giordanetto, F.; Medda, F. DYRK1A inhibition as potential treatment for Alzheimer's disease. *Future Med. Chem.* **2016**, *8*, 681−696.
(34) Branca, C.; Shaw, D. M.; Belfiore, R.; Gokhale, V.; Shaw, A. Y.; Foley, C.; Smith, B.; Hulme, C.; Dunckley, T.; Meechoovet, B.; Caccamo, A.; Oddo, S. Dyrk1 inhibition improves Alzheimer's disease-like pathology. *Aging Cell* **2017**, *16*, 1146−1154.
(35) García-Cerro, S.; Rueda, N.; Vidal, V.; Lantigua, S.; Martínez-Cué, C. Normalizing the Gene Dosage of Dyrk1A in a Mouse Model of Down Syndrome Rescues Several Alzheimer's Disease Phenotypes. *Neurobiol. Dis.* **2017**, *106*, 76−88.
(36) Jarhad, D. B.; Mashelkar, K. K.; Kim, H.-R.; Noh, M.; Jeong, L. S. Dual-specificity tyrosine phosphorylation-regulated kinase 1A (DYRK1A) inhibitors as potential therapeutics. *J. Med. Chem.* **2018**, *61*, 9791−9810.
(37) Velazquez, R.; Meechoovet, B.; Ow, A.; Foley, C.; Shaw, A.; Smith, B.; Oddo, S.; Hulme, C.; Dunckley, T. Chronic Dyrk1 inhibition delays the onset of AD-Like pathology in 3xTg-AD mice. *Mol. Neurobiol.* **2019**, *56*, 8364−8375.
(38) Melchior, B.; Mittapalli, G. K.; Lai, C.; Duong-Polk, K.; Stewart, J.; Güner, B.; Hofilena, B.; Tjitro, A.; Anderson, S. D.; Herman, D. S.; Dellamary, L.; Swearingen, C. J.; Sunil, K. C.; Yazici, Y. Tau pathology reduction with SM07883, a novel, potent, and selective oral DYRK1A inhibitor: A potential therapeutic for Alzheimer's disease. *Aging Cell* **2019**, *18*, No. e13000.
(39) Souchet, B.; Audrain, M.; Billard, J. M.; Dairou, J.; Fol, R.; Orefice, N. S.; Tada, S.; Gu, Y.; Dufayet-Chaffaud, G.; Limanton, E.; Carreaux, F.; Bazureau, J. P.; Alves, S.; Meijer, L.; Janel, N.; Braudeau, J.; Cartier, N. Inhibition of DYRK1A proteolysis modifies its kinase specificity and rescues Alzheimer phenotype in APP/PS1 mice. *Acta Neuropathol. Commun.* **2019**, *7*, 46.
(40) Cen, L.; Xiao, Y.; Wei, L.; Mo, M.; Chen, X.; Li, S.; Yang, X.; Huang, Q.; Qu, S.; Pei, Z.; Xu, P. Association of DYRK1A polymorphisms with sporadic Parkinson's disease in Chinese Han population. *Neurosci. Lett.* **2016**, *632*, 39−43.
(41) Chiu, C. C.; Yeh, T. H.; Chen, R. S.; Chen, H. C.; Huang, Y. Z.; Weng, Y. H.; Cheng, Y. C.; Liu, Y. C.; Cheng, A. J.; Lu, Y. C.; Chen, Y. J.; Lin, Y. W.; Hsu, C. C.; Chen, Y. L.; Lu, C. S.; Wang, H. L. Upregulated expression of microRNA-204−5p leads to the death of dopaminergic Cells by targeting DYRK1A-mediated apoptotic signaling cascade. *Front. Cell. Neurosci.* **2019**, *13*, 399.
(42) Nalls, M. A.; Blauwendraat, C.; Vallerga, C. L.; Heilbron, K.; Bandres-Ciga, S.; Chang, D.; Tan, M.; Kia, D. A.; Noyce, A. J.; Xue, A.; Bras, J.; Young, E.; von Coelln, R.; Simón-Sánchez, J.; Schulte, C.; Sharma, M.; Krohn, L.; Pihlstrøm, L.; Siitonen, A.; Iwaki, H.; Leonard, H.; Faghri, F.; Gibbs, J. R.; Hernandez, D. G.; Scholz, S. W.; Botia, J. A.; Martinez, M.; Corvol, J. C.; Lesage, S.; Jankovic, J.; Shulman, L. M.; Sutherland, M.; Tienari, P.; Majamaa, K.; Toft, M.; Andreassen, O. A.; Bangale, T.; Brice, A.; Yang, J.; Gan-Or, Z.; Gasser, T.; Heutink, P.; Shulman, J. M.; Wood, N. W.; Hinds, D. A.; Hardy, J. A.; Morris, H. R.; Gratten, J.; Visscher, P. M.; Graham, R. R.; Singleton, A. B.; et al. 23andMe Research Team; System Genomics of Parkinson's Disease Consortium; International Parkinson's Disease Genomics Consortium. Identification of novel risk loci, causal insights, and heritable risk for Parkinson's disease: a meta-analysis

https://doi.org/10.1021/acs.jmedchem.1c01141
J. Med. Chem. 2022, 65, 1396−1417

of genome-wide association studies. *Lancet Neurol.* **2019**, *18*, 1091−1102.
(43) Wang, P.; Alvarez-Perez, J. C.; Felsenfeld, D. P.; Liu, H.; Sivendran, S.; Bender, A.; Kumar, A.; Sanchez, R.; Scott, D. K.; Garcia-Ocaña, A.; Stewart, A. F. A high-throughput chemical screen reveals that harmine-mediated inhibition of DYRK1A increases human pancreatic beta cell replication. *Nat. Med.* **2015**, *21*, 383−388.
(44) Dirice, E.; Walpita, D.; Vetere, A.; Meier, B. C.; Kahraman, S.; Hu, J.; Dančík, V.; Burns, S. M.; Gilbert, T. J.; Olson, D. E.; Clemons, P. A.; Kulkarni, R. N.; Wagner, B. K. Inhibition of DYRK1A stimulates human β-cell proliferation. *Diabetes* **2016**, *65*, 1660−1671.
(45) Shen, W.; Taylor, B.; Jin, Q.; Nguyen-Tran, V.; Meeusen, S.; Zhang, Y. Q.; Kamireddy, A.; Swafford, A.; Powers, A. F.; Walker, J.; Lamb, J.; Bursalaya, B.; DiDonato, M.; Harb, G.; Qiu, M.; Filippi, C. M.; Deaton, L.; Turk, C. N.; Suarez-Pinzon, W. L.; Liu, Y.; Hao, X.; Mo, T.; Yan, S.; Li, J.; Herman, A. E.; Hering, B. J.; Wu, T.; Martin Seidel, H.; McNamara, P.; Glynne, R.; Laffitte, B. Inhibition of DYRK1A and GSK3B induces human β-cell proliferation. *Nat. Commun.* **2015**, *6*, 8372.
(46) Belgardt, B. F.; Lammert, E. DYRK1A: A promising drug target for islet transplant-based diabetes therapies. *Diabetes* **2016**, *65*, 1496−1498.
(47) Kumar, K.; Wang, P.; Sanchez, R.; Swartz, E. A.; Stewart, A. F.; DeVita, R. J. Development of kinase-selective, harmine-based DYRK1A inhibitors that induce pancreatic human β-cell proliferation. *J. Med. Chem.* **2018**, *61*, 7687−7699.
(48) Abdolazimi, Y.; Zhao, Z.; Lee, S.; Xu, H.; Allegretti, P.; Horton, T. M.; Yeh, B.; Moeller, H. P.; Nichols, R. J.; McCutcheon, D.; Shalizi, A.; Smith, M.; Armstrong, N. A.; Annes, J. P. CC-401 Promotes β-cell replication via pleiotropic consequences of DYRK1A/B inhibition. *Endocrinology* **2018**, *159*, 3143−3157.
(49) Tian, S.; Jia, W.; Lu, M.; Zhao, J.; Sun, X. Dual-specificity tyrosine phosphorylation-regulated kinase 1A ameliorates insulin resistance in neurons by up-regulating IRS-1 expression. *J. Biol. Chem.* **2019**, *294*, 20164−20176.
(50) Wang, P.; Karakose, E.; Liu, H.; Swartz, E.; Ackeifi, C.; Zlatanic, V.; Wilson, J.; González, B. J.; Bender, A.; Takane, K. K.; Ye, L.; Harb, G.; Pagliuca, F.; Homann, D.; Egli, D.; Argmann, C.; Scott, D. K.; Garcia-Ocaña, A.; Stewart, A. F. Combined inhibition of DYRK1A, SMAD, and Trithorax pathways synergizes to induce robust replication in adult human beta cells. *Cell Metab.* **2019**, *29*, P638.
(51) Ackeifi, C.; Swartz, E.; Kumar, K.; Liu, H.; Chalada, S.; Karakose, E.; Scott, D. K.; Garcia-Ocaña, A.; Sanchez, R.; DeVita, R. J.; Stewart, A. F.; Wang, P. Pharmacologic and genetic approaches define human pancreatic β cell mitogenic targets of DYRK1A inhibitors. *JCI Insight* **2020**, *5*, No. e132594.
(52) Kumar, K.; Suebsuwong, C.; Wang, P.; Garcia-Ocana, A.; Stewart, A. F.; DeVita, R. J. DYRK1A inhibitors as potential therapeutics for β-cell regeneration for diabetes. *J. Med. Chem.* **2021**, *64*, 2901−2922.
(53) Deshmukh, V.; O'Green, A. L.; Bossard, C.; Seo, T.; Lamangan, L.; Ibanez, M.; Ghias, A.; Lai, C.; Do, L.; Cho, S.; Cahiwat, J.; Chiu, K.; Pedraza, M.; Anderson, S.; Harris, R.; Dellamary, L.; Kc, S.; Barroga, C.; Melchior, B.; Tam, B.; Kennedy, S.; Tambiah, J.; Hood, J.; Yazici, Y. Modulation of the Wnt pathway through inhibition of CLK2 and DYRK1A by Lorecivivint as a novel, potentially disease-modifying approach for knee osteoarthritis treatment. *Osteoarthr. Cartil.* **2019**, *27*, 1347−1360.
(54) Yazici, Y.; McAlindon, T. E.; Gibofsky, A.; Lane, N. E.; Lattermann, C.; Skrepnik, N.; Swearingen, C. J.; Simsek, I.; Ghandehari, H.; DiFrancesco, A.; Gibbs, J.; Tambiah, J. R. S.; Hochberg, M. C. A phase 2b randomized trial of Lorecivivint, a novel intra-articular CLK2/DYRK1A inhibitor and Wnt pathway modulator for knee osteoarthritis. *Osteoarthr. Cartil.* **2021**, *29*, 654−666.
(55) Deshmukh, V.; Seo, T.; Lauren O'Green, A.; Ibanez, M.; Hofilena, B.; Sunil, K.; Stewart, J.; Dellamary, L.; Chiu, K.; Ghias, A.; Barroga, C.; Kennedy, S.; Tambiah, J.; Hood, J.; Yazici, Y. SM04755, a small-molecule inhibitor of the Wnt pathway, as a potential topical treatment for tendinopathy. *J. Orthop. Res.* **2021**, *39*, 2048.
(56) Bol, S. M.; Moerland, P. D.; Limou, S.; van Remmerden, Y.; Coulonges, C.; van Manen, D.; Herbeck, J. T.; Fellay, J.; Sieberer, M.; Sietzema, J. G.; van 't Slot, R.; Martinson, J.; Zagury, J. F.; Schuitemaker, H.; van 't Wout, A. B. Genome-wide association study identifies single nucleotide polymorphism in DYRK1A associated with replication of HIV-1 in monocyte-derived macrophages. *PLoS One* **2011**, *6*, No. e17190.
(57) Booiman, T.; Loukachov, V. V.; van Dort, K. A.; van 't Wout, A. B.; Kootstra, N. A. DYRK1A Controls HIV-1 Replication at a transcriptional level in an NFAT dependent manner. *PLoS One* **2015**, *10*, No. e0144229.
(58) Hamilton, S. T.; Hutterer, C.; Egilmezer, E.; Steingruber, M.; Milbradt, J.; Marschall, M.; Rawlinson, W. D. Human cytomegalovirus utilises cellular dual-specificity tyrosine phosphorylation-regulated kinases during placental replication. *Placenta* **2018**, *72*, 10−19.
(59) Kisaka, J. K.; Ratner, L.; Kyei, G. B. The dual-specificity kinase DYRK1A modulates the levels of cyclin L2 to control HIV replication in macrophages. *J. Virol.* **2020**, *94*, e01583-19.
(60) Dirmeier, S.; Dächert, C.; van Hemert, M.; Tas, A.; Ogando, N. S.; van Kuppeveld, F.; Bartenschlager, R.; Kaderali, L.; Binder, M.; Beerenwinkel, N. Host factor prioritization for pan-viral genetic perturbation screens using random intercept models and network propagation. *PLoS Comput. Biol.* **2020**, *16*, No. e1007587.
(61) Lee, P.; Bhansali, R.; Izraeli, S.; Hijiya, N.; Crispino, J. D. The biology, pathogenesis and clinical aspects of Acute Lymphoblastic Leukemia in children with Down syndrome. *Leukemia* **2016**, *30*, 1816−1823.
(62) Bhansali, R. S.; Rammohan, M.; Lee, P.; Laurent, A. P.; Wen, Q.; Suraneni, P.; Yip, B. H.; Tsai, Y.-C.; Jenni, S.; Bornhauser, B.; Siret, A.; Fruit, C.; Pacheco-Benichou, A.; Harris, E.; Besson, T.; Thompson, B. J.; Goo, Y. A.; Hijiya, N.; Vilenchik, M.; Izraeli, S.; Bourquin, J. P.; Malinge, S.; Crispino, J. D. DYRK1A regulates B cell Acute Lymphoblastic Leukemia through phosphorylation of FOXO1 and STAT3. *J. Clin. Invest.* **2021**, *131*, No. e135937.
(63) Malinge, S.; Bliss-Moreau, M.; Kirsammer, G.; Diebold, L.; Chlon, T.; Gurbuxani, S.; Crispino, J. D. Increased dosage of the chromosome 21 ortholog Dyrk1a promotes Megakaryoblastic Leukemia in a murine model of Down syndrome. *J. Clin. Invest.* **2012**, *122*, 948−962.
(64) Laham, A. J.; Saber-Ayad, M.; El-Awady, R. DYRK1A: A Down syndrome-related dual protein kinase with a versatile role in tumorigenesis. *Cell. Mol. Life Sci.* **2021**, *78*, 603−619.
(65) Pozo, N.; Zahonero, C.; Fernández, P.; Liñares, J. M.; Ayuso, A.; Hagiwara, M.; Pérez, A.; Ricoy, J. R.; Hernández-Laín, A.; Sepúlveda, J. M.; Sánchez-Gómez, P. Inhibition of DYRK1A destabilizes EGFR and reduces EGFR-dependent glioblastoma growth. *J. Clin. Invest.* **2013**, *123*, 2475−2487.
(66) Luna, J.; Boni, J.; Cuatrecasas, M.; Bofill-De Ros, X.; Núñez-Manchón, E.; Gironella, M.; Vaquero, E. C.; Arbones, M. L.; de la Luna, S.; Fillat, C. DYRK1A modulates C-MET in pancreatic ductal adenocarcinoma to drive tumour growth. *Gut* **2019**, *68*, 1465−1476.
(67) Bai, Z.; Du, Y.; Cong, L.; Cheng, Y. The USP22 Promotes the growth of cancer cells through the DYRK1A in pancreatic ductal adenocarcinoma. *Gene* **2020**, *758*, 144960.
(68) Zhao, C.; Wang, D.; Gao, Z.; Kan, H.; Qiu, F.; Chen, L.; Li, H. Licocoumarone induces BxPC-3 pancreatic adenocarcinoma cell death by inhibiting DYRK1A. *Chem.-Biol. Interact.* **2020**, *316*, 108913.
(69) Nguyen, T. L.; Fruit, C.; Hérault, Y.; Meijer, L.; Besson, T. Dual-specificity tyrosine phosphorylation-regulated kinase 1A (DYRK1A) inhibitors: a survey of recent patent literature. *Expert Opin. Ther. Pat.* **2017**, *27*, 1183−1199.
(70) Ortiz-Abalia, J.; Sahún, I.; Altafaj, X.; Andreu, N.; Estivill, X.; Dierssen, M.; Fillat, C. Targeting Dyrk1A with AAVshRNA attenuates motor alterations in TgDyrk1A, a mouse model of Down syndrome. *Am. J. Hum. Genet.* **2008**, *83*, 479−488.
(71) Altafaj, X.; Martín, E. D.; Ortiz-Abalia, J.; Valderrama, A.; Lao-Peregrín, C.; Dierssen, M.; Fillat, C. Normalization of Dyrk1A expression by AAV2/1-shDyrk1A attenuates hippocampal-dependent

https://doi.org/10.1021/acs.jmedchem.1c01141
J. Med. Chem. 2022, 65, 1396−1417

defects in the Ts65Dn mouse model of Down syndrome. *Neurobiol. Dis.* **2013**, *52*, 117−127.
(72) Naert, G.; Ferré, V.; Meunier, J.; Keller, E.; Malmström, S.; Givalois, L.; Carreaux, F.; Bazureau, J. P.; Maurice, T. Leucettine L41, a DYRK1A-preferential DYRKs/CLKs inhibitor, prevents memory impairments and neurotoxicity induced by oligomeric Aβ25−35 peptide administration in mice. *Eur. Neuropsychopharmacol.* **2015**, *25*, 2170−2182.
(73) Neumann, F.; Gourdain, S.; Albac, C.; Dekker, A. D.; Bui, L. C.; Dairou, J.; Schmitz-Afonso, I.; Hue, N.; Rodrigues-Lima, F.; Delabar, J.-M.; Potier, M.-C.; Le Caër, J.-P.; Touboul, D.; Delatour, B.; Cariou, K.; Dodd, R. H. DYRK1A inhibition and cognitive rescue in a Down syndrome mouse model are induced by new fluoro-DANDY derivatives. *Sci. Rep.* **2018**, *8*, 2859.
(74) De Toma, I.; Ortega, M.; Aloy, P.; Sabidó, E.; Dierssen, M. DYRK1A Overexpression alters cognition and neural-related proteomic pathways in the hippocampus that are rescued by green tea extract and/or environmental enrichment. *Front. Mol. Neurosci.* **2019**, *12*, 272.
(75) Souchet, B.; Duchon, A.; Gu, Y.; Dairou, J.; Chevalier, C.; Daubigney, F.; Nalesso, V.; Créau, N.; Yu, Y.; Janel, N.; Herault, Y.; Delabar, J.-M. Prenatal treatment with EGCG enriched green tea extract rescues GAD67 related developmental and cognitive defects in Down syndrome mouse models. *Sci. Rep.* **2019**, *9*, 3914.
(76) Chan, G. W.; Mong, S.; Hemling, M. E.; Freyer, A. J.; Offen, P. H.; DeBrosse, C. W.; Sarau, H. M.; Westley, J. W. New leukotriene B4 receptor antagonist: leucettamine A and related imidazole alkaloids from the marine sponge *Leucetta microraphis*. *J. Nat. Prod.* **1993**, *56*, 116−121.
(77) Roué, N.; Bergman, J. Synthesis of the marine alkaloid leucettamine B. *Tetrahedron* **1999**, *55*, 14729−14738.
(78) Watanabe, K.; Tsuda, Y.; Iwashima, M.; Iguchi, K. A new bioactive triene aldehyde from the marine sponge *Leucetta microraphis*. *J. Nat. Prod.* **2000**, *63*, 258−260.
(79) Roué, M.; Quévrain, E.; Domart-Coulon, I.; Bourguet-Kondracki, M. L. Assessing calcareous sponges and their associated bacteria for the discovery of new bioactive natural products. *Nat. Prod. Rep.* **2012**, *29*, 739−751.
(80) Loaëc, N.; Attanasio, E.; Villiers, B.; Durieu, E.; Tahtouh, T.; Cam, M.; Davis, R. A.; Alencar, A.; Roué, M.; Bourguet-Kondracki, M. L.; Proksch, P.; Limanton, E.; Guiheneuf, S.; Carreaux, F.; Bazureau, J. P.; Klautau, M.; Meijer, L. Marine derived 2-aminoimidazolone alkaloids. Leucettamine B-related polyandrocarpamines inhibit mammalian and protozoan DYRK &/CLK kinases. *Mar. Drugs* **2017**, *15*, 316.
(81) Debdab, M.; Carreaux, F.; Renault, S.; Soundararajan, M.; Fedorov, O.; Filippakopoulos, P.; Lozach, O.; Babault, L.; Tahtouh, T.; Baratte, B.; Ogawa, Y.; Hagiwara, M.; Eisenreich, A.; Rauch, U.; Knapp, S.; Meijer, L.; Bazureau, J.-P. Leucettines, a class of potent inhibitors of cdc2-like kinases and dual specificity, tyrosine phosphorylation regulated kinases derived from the marine sponge leucettamine B: modulation of alternative pre-RNA splicing. *J. Med. Chem.* **2011**, *54*, 4172−4186.
(82) Tahtouh, T.; Elkins, J. M.; Filippakopoulos, P.; Soundararajan, M.; Burgy, G.; Durieu, E.; Cochet, C.; Schmid, R. S.; Lo, D. C.; Delhommel, F.; Oberholzer, A. E.; Pearl, L. H.; Carreaux, F.; Bazureau, J. P.; Knapp, S.; Meijer, L. Selectivity, cocrystal structures and neuroprotective properties of leucettines, a family of protein kinase inhibitors derived from the marine sponge alkaloid leucettamine B. *J. Med. Chem.* **2012**, *55*, 9312−9330.
(83) Fant, X.; Durieu, E.; Chicanne, G.; Payrastre, B.; Sbrissa, D.; Shisheva, A.; Limanton, E.; Carreaux, F.; Bazureau, J. P.; Meijer, L. Cdc-like/dual-specificity tyrosine phosphorylation-regulated kinases Leucettine L41 induces mTOR-dependent autophagy: implication for Alzheimer's disease. *Mol. Pharmacol.* **2014**, *85*, 441−450.
(84) Burgy, G.; Tahtouh, T.; Durieu, E.; Foll-Josselin, B.; Limanton, E.; Meijer, L.; Carreaux, F.; Bazureau, J. P. Chemical synthesis and biological validation of immobilized kinase inhibitory Leucettines. *Eur. J. Med. Chem.* **2013**, *62C*, 728−737.
(85) Molina, P.; Almendros, P.; Fresneda, P. M. An iminophosphorane-mediated efficient synthesis of the alkaloid leucettamine B of marine of origin. *Tetrahedron Lett.* **1994**, *35*, 2235−2236.
(86) Sechi, M.; Derudas, M.; Dallocchio, R.; Dessì, A.; Bacchi, A.; Sannia, L.; Carta, F.; Palomba, M.; Ragab, O.; Chan, C.; Shoemaker, R.; Sei, S.; Dayam, R.; Neamati, N. Design and synthesis of novel indole beta-diketo acid derivatives as HIV-1 integrase inhibitors. *J. Med. Chem.* **2004**, *47*, 5298−5310.
(87) Stokes, B. J.; Dong, H.; Leslie, B. E.; Pumphrey, A. L.; Driver, T. G. Intramolecular C-H amination reactions:exploitation of the Rh2 (II)-catalyzeddecomposition of azidoacrylates. *J. Am. Chem. Soc.* **2007**, *129* (24), 7500−7501.
(88) Shi, J.; Zhang, T.; Zhou, C.; Chohan, M. O.; Gu, X.; Wegiel, J.; Zhou, J.; Hwang, Y. W.; Iqbal, K.; Grundke-Iqbal, I.; Gong, C. X.; Liu, F. Increased dosage of Dyrk1A alters alternative splicing factor (ASF)-regulated alternative splicing of tau in Down syndrome. *J. Biol. Chem.* **2008**, *283*, 28660−28669.
(89) Long, J. C.; Caceres, J. F. The SR protein family of splicing factors: master regulators of gene expression. *Biochem. J.* **2009**, *417*, 15−27.
(90) de Graaf, K.; Czajkowska, H.; Rottmann, S.; Packman, L. C.; Lilischkis, R.; Lüscher, B.; Becker, W. The protein kinase DYRK1A phosphorylates the splicing factor SF3b1/SAP155 at Thr434, a novel in vivo phosphorylation. *BMC Biochem* **2006**, *7*, 7.
(91) Qian, W.; Liang, H.; Shi, J.; Jin, N.; Grundke-Iqbal, I.; Iqbal, K.; Gong, C. X.; Liu, F. Regulation of the alternative splicing of tau exon 10 by SC35 and Dyrk1A. *Nucleic Acids Res.* **2011**, *39*, 6161−6171.
(92) Ding, S.; Shi, J.; Qian, W.; Iqbal, K.; Grundke-Iqbal, I.; Gong, C. X.; Liu, F. Regulation of alternative splicing of tau exon 10 by 9G8 and Dyrk1A. *Neurobiol. Aging* **2012**, *33*, 1389−1399.
(93) Yin, X.; Jin, N.; Gu, J.; Shi, J.; Zhou, J.; Gong, C.-X.; Iqbal, K.; Grundke-Iqbal, I.; Liu, F. Dual-specificity tyrosine phosphorylation-regulated kinase 1A (Dyrk1A) modulates Serine/Arginine-Rich Protein 55 (SRp55)-promoted Tau exon 10 inclusion. *J. Biol. Chem.* **2012**, *287*, 30497−30506.
(94) Schmitt, C.; Miralinaghi, P.; Mariano, M.; Hartmann, R. W.; Engel, M. Hydroxybenzothiophene Ketones Are Efficient Pre-mRNA Splicing modulators due to dual inhibition of Dyrk1A and Clk1/4. *ACS Med. Chem. Lett.* **2014**, *5*, 963−967.
(95) He, J.; Yao, J.; Sheng, H.; Zhu, J. Involvement of the dual-specificity tyrosine phosphorylation-regulated kinase 1A-alternative splicing factor-calcium/calmodulin-dependent protein kinase IIδ signaling pathway in myocardial infarction-induced heart failure of rats. *J. Card. Failure* **2015**, *21*, 751−760.
(96) Lu, S.; Yin, X. Overexpression of Dyrk1A regulates cardiac troponin T splicing in cells and mice. *Biochem. Biophys. Res. Commun.* **2016**, *473*, 993−998.
(97) Yin, X.; Jin, N.; Shi, J.; Zhang, Y.; Wu, Y.; Gong, C.-X.; Iqbal, K.; Liu, F. Dyrk1A Overexpression leads to increase of 3R-Tau expression and cognitive deficits in Ts65Dn Down syndrome mice. *Sci. Rep.* **2017**, *7*, 619.
(98) Muraki, M.; Ohkawara, B.; Hosoya, T.; Onogi, H.; Koizumi, J.; Koizumi, T.; Sumi, K.; Yomoda, J.; Murray, M. V.; Kimura, H.; Furuichi, K.; Shibuya, H.; Krainer, A. R.; Suzuki, M.; Hagiwara, M. Manipulation of alternative splicing by a newly developed inhibitor of Clks. *J. Biol. Chem.* **2004**, *279*, 24246−24254.
(99) Yomoda, J.; Muraki, M.; Kataoka, N.; Hosoya, T.; Suzuki, M.; Hagiwara, M.; Kimura, H. Combination of Clk family kinase and SRp75 modulates alternative splicing of Adenovirus E1A. *Genes Cells* **2008**, *13*, 233−244.
(100) Uzor, S.; Zorzou, P.; Bowler, E.; Porazinski, S.; Wilson, I.; Ladomery, M. Autoregulation of the human splice factor kinase CLK1 through exon skipping and intron retention. *Gene* **2018**, *670*, 46−54.
(101) Wegmann, S.; Biernat, J.; Mandelkow, E. A current view on Tau protein phosphorylation in Alzheimer's disease. *Curr. Opin. Neurobiol.* **2021**, *69*, 131−138.
(102) Woods, Y. L.; Cohen, P.; Becker, W.; Jakes, R.; Goedert, M.; Wang, X.; Proud, C. G. The kinase DYRK phosphorylates protein-synthesis initiation factor eIF2Bepsilon at Ser539 and the micro-

https://doi.org/10.1021/acs.jmedchem.1c01141
J. Med. Chem. 2022, 65, 1396−1417

tubule-associated protein tau at Thr212: potential role for DYRK as a glycogen synthase kinase 3-priming kinase. *Biochem. J.* **2001**, *355*, 609−615.
(103) Ryoo, S. R.; Jeong, H. K.; Radnaabazar, C.; Yoo, J. J.; Cho, H. J.; Lee, H. W.; Kim, I. S.; Cheon, Y. H.; Ahn, Y. S.; Chung, S. H.; Song, W. J. DYRK1A-mediated hyperphosphorylation of Tau. A functional link between Down syndrome and Alzheimer disease. *J. Biol. Chem.* **2007**, *282*, 34850−34857.
(104) Chen, S.; Townsend, K.; Goldberg, T. E.; Davies, P.; Conejero-Goldberg, C. MAPT isoforms: differential transcriptional profiles related to 3R and 4R splice variants. *J. Alzheimer's Dis.* **2011**, *22*, 1313−1329.
(105) Flament, S.; Delacourte, A.; Mann, D. M. Phosphorylation of Tau proteins: a major event during the process of neurofibrillary degeneration. A comparative study between Alzheimer's disease and Down's syndrome. *Brain Res.* **1990**, *516*, 15−19.
(106) Hanger, D. P.; Brion, J. P.; Gallo, J. M.; Cairns, N. J.; Luthert, P. J.; Anderton, B. H. Tau in Alzheimer's disease and Down's syndrome is insoluble and abnormally phosphorylated. *Biochem. J.* **1991**, *275*, 99−104.
(107) Goedert, M.; Spillantini, M. G.; Cairns, N. J.; Crowther, R. A. Tau proteins of Alzheimer paired helical filaments: abnormal phosphorylation of all six brain isoforms. *Neuron* **1992**, *8*, 159−168.
(108) Liu, F.; Liang, Z.; Wegiel, J.; Hwang, Y. W.; Iqbal, K.; Grundke-Iqbal, I.; Ramakrishna, N.; Gong, C. X. Overexpression of Dyrk1A contributes to neurofibrillary degeneration in Down syndrome. *FASEB J.* **2008**, *22*, 3224−3233.
(109) Mondragón-Rodríguez, S.; Perry, G.; Luna-Muñoz, J.; Acevedo-Aquino, M. C.; Williams, S. Phosphorylation of tau protein at sites Ser(396−404) is one of the earliest events in Alzheimer's disease and Down syndrome. *Neuropathol. Appl. Neurobiol.* **2014**, *40*, 121−135.
(110) Tatebe, H.; Kasai, T.; Ohmichi, T.; Kishi, Y.; Kakeya, T.; Waragai, M.; Kondo, M.; Allsop, D.; Tokuda, T. Quantification of plasma phosphorylated tau to use as a biomarker for brain Alzheimer pathology: pilot case-control studies including patients with Alzheimer's disease and down syndrome. *Mol. Neurodegener.* **2017**, *12*, 63.
(111) Fortea, J.; Vilaplana, E.; Carmona-Iragui, M.; Benejam, B.; Videla, L.; Barroeta, I.; Fernández, S.; Altuna, M.; Pegueroles, J.; Montal, V.; Valldeneu, S.; Giménez, S.; González-Ortiz, S.; Muñoz, L.; Estellés, T.; Illán-Gala, I.; Belbin, O.; Camacho, V.; Wilson, L. R.; Annus, T.; Osorio, R. S.; Videla, S.; Lehmann, S.; Holland, A. J.; Alcolea, D.; Clarimón, J.; Zaman, S. H.; Blesa, R.; Lleó, A. Clinical and biomarker changes of Alzheimer's disease in adults with Down syndrome: a cross-sectional study. *Lancet* **2020**, *395*, 1988−1997.
(112) Sun, Q. Z.; Lin, G. F.; Li, L. L.; Jin, X. T.; Huang, L. Y.; Zhang, G.; Yang, W.; Chen, K.; Xiang, R.; Chen, C.; Wei, Y. Q.; Lu, G. W.; Yang, S. Y. Discovery of potent and selective inhibitors of Cdc2-Like Kinase 1 (CLK1) as a new class of autophagy inducers. *J. Med. Chem.* **2017**, *60*, 6337−6352.
(113) Zhang, Y.; Xia, A.; Zhang, S.; Lin, G.; Liu, J.; Chen, P.; Mu, B.; Jiao, Y.; Xu, W.; Chen, M.; Li, L. Discovery of 3,6-disubstutited-imidazo[1,2-a]pyridine derivatives as a new class of CLK1 inhibitors. *Bioorg. Med. Chem. Lett.* **2021**, *41*, 127881.
(114) Gregory, K. J.; Dong, E. N.; Meiler, J.; Conn, P. J. Allosteric modulation of metabotropic glutamate receptors: structural insights and therapeutic potential. *Neuropharmacology* **2011**, *60*, 66−81.
(115) Ahn, K. H.; Mahmoud, M. M.; Kendall, D. A. Allosteric modulator ORG27569 induces CB1 cannabinoid receptor high affinity agonist binding state, receptor internalization, and Gi protein-independent ERK1/2 kinase activation. *J. Biol. Chem.* **2012**, *287*, 12070−12082.
(116) Ahn, K. H.; Mahmoud, M. M.; Shim, J. Y.; Kendall, D. A. Distinct roles of beta-arrestin 1 and beta-arrestin 2 in ORG27569-induced biased signaling and internalization of the cannabinoid receptor 1 (CB1). *J. Biol. Chem.* **2013**, *288*, 9790−9800.
(117) Navarro-Romero, A.; Vázquez-Oliver, A.; Gomis-González, M.; Garzón-Montesinos, C.; Falcón-Moya, R.; Pastor, A.; Martín-García, E.; Pizarro, N.; Busquets-Garcia, A.; Revest, J. M.; Piazza, P. V.; Bosch, F.; Dierssen, M.; de la Torre, R.; Rodríguez-Moreno, A.; Maldonado, R.; Ozaita, A. Cannabinoid type-1 receptor blockade restores neurological phenotypes in two models for Down syndrome. *Neurobiol. Dis.* **2019**, *125*, 92−106.

https://doi.org/10.1021/acs.jmedchem.1c01141
J. Med. Chem. 2022, 65, 1396−1417